A cooperative strategy for optimizing vehicle relocations and staff movements in cities where several carsharing companies operate simultaneously

Chang, Ximing; Wu, Jianjun; Correia, Gonçalo Homem de Almeida; Sun, Huijun; Feng, Ziyan

DOI
10.1016/j.tre.2022.102711

Publication date
2022

Document Version
Final published version

Published in
Transportation Research Part E: Logistics and Transportation Review

Citation (APA)
Chang, X., Wu, J., Correia, G. H. D. A., Sun, H., & Feng, Z. (2022). A cooperative strategy for optimizing vehicle relocations and staff movements in cities where several carsharing companies operate simultaneously. *Transportation Research Part E: Logistics and Transportation Review*, *161*, Article 102711. https://doi.org/10.1016/j.tre.2022.102711

Transportation Research Part E 161 (2022) 102711

Contents lists available at ScienceDirect

Transportation Research Part E

journal homepage: www.elsevier.com/locate/tre

A cooperative strategy for optimizing vehicle relocations and staff movements in cities where several carsharing companies operate simultaneously

Ximing Chang [a], Jianjun Wu [a,b,*], Gonçalo Homem de Almeida Correia [c], Huijun Sun [d], Ziyan Feng [a]

[a] State Key Laboratory of Rail Traffic Control and Safety, Beijing Jiaotong University, Beijing, China
[b] Key Laboratory of Transport Industry of Big Data Application Technologies for Comprehensive Transport, Ministry of Transport, Beijing Jiaotong University, Beijing, China
[c] Department of Transport & Planning, Delft University of Technology, Delft, the Netherlands
[d] School of Traffic and Transportation, Beijing Jiaotong University, Beijing, China

ARTICLE INFO

Keywords:
One-way carsharing
Multi-step demand forecasting
Graph convolutional network
Cooperative relocation
Staff rebalancing

ABSTRACT

Carsharing has become a popular travel mode owing to its convenience of use, easy parking, and low cost of using a car by those who only need it occasionally. However, because of the inadequate location of carsharing stations (station-based systems) or vehicles (free-floating systems), effectively requiring expensive and complex relocation strategies, a number of customers are lost, and some carsharing companies are facing bankruptcy. This study proposes a data-driven, dynamic, multi-company relocation method, which aims to reduce relocation costs and increase profit in one-way carsharing station-based systems through cooperative strategies. The method starts from the prediction of carsharing inflows and outflows at each station throughout the day using a new deep learning algorithm designated as "the attention-enhanced temporal graph convolutional network". It adopts an encoder-decoder structure to simultaneously capture the temporal and spatial carsharing usage patterns. A two-phase integer programming model is proposed to optimize the process of vehicle relocation and staff rebalancing with cooperative relocation strategies: the sharing of relocation staff, the sharing of vehicles and stations among the different companies. An adaptive large neighborhood search based heuristic approach is implemented to solve the two-phase model. Based on the 6-month travel records from four carsharing companies operating simultaneously in Fuzhou, China, the proposed model and cooperative strategies are assessed. The results show that the total profit of the four carsharing companies can be increased by 25.49% with the cooperation of staff and vehicles. In addition, we prospect the future relocation with automated vehicles, whereby the profit can be increased by 46.69% without the need to employ the relocation staff.

1. Introduction

The rapid development of cities has caused a high travel demand for car usage (Wan et al., 2021). However, in big cities, the cost of

* Corresponding author at: State Key Laboratory of Rail Traffic Control and Safety, Beijing Jiaotong University, Beijing, China.
E-mail address: jjwu1@bjtu.edu.cn (J. Wu).

https://doi.org/10.1016/j.tre.2022.102711
Received 4 June 2021; Received in revised form 5 February 2022; Accepted 2 April 2022
Available online 12 April 2022
1366-5545/

car usage is increasing, coupled with parking problems, traffic congestion, and restrictions on private car usage such as the odd–even license plate rule (Shaheen, et al., 2015; Jian et al., 2020; Zeng et al., 2021). Carsharing is an emerging travel mode that allows people who want to rent cars for short periods and pay for their usage based on the travel distance and duration. Carsharing is poised to meet people's urban travel demand by sharing the same vehicle, which improves vehicle usage frequency and leads to reduced car ownership (Klincevicius et al., 2014). Currently, carsharing systems are growing in cities because they provide a cheaper alternative than buying a vehicle and are more flexible than public transport (Shaheen and Cohen, 2013; Sprei et al., 2019). Shared cars and stations (in station-based systems) are distributed around residential communities, commercial office areas, university towns, etc. to meet people's daily travel demands. In China, carsharing services have sprung up and flourished. Till 2018, more than 500 carsharing companies were registered, with more than 100,000 vehicles offering the services (Sohu News, 2018). Modern carsharing systems use existing resources to achieve a higher matching efficiency between people and vehicles through advanced technologies, thereby reducing congestion, pollution, and parking spaces in cities. Chen and Kockelman (2016) illustrated that greenhouse gas emissions are reduced by approximately 51% when travelers adopt carsharing.

Carsharing systems can be divided into round-trip systems and one-way systems (Jorge et al., 2014). In one-way carsharing systems, users can pick up shared cars at one station and return them to another. The one-way system enhances the service level for the users (Efthymiou et al., 2012). However, because of the imbalance in demand in both time and space, the problem of vehicle stock shortage or lack of parking space may occur at some stations throughout the day (Jian et al., 2016b; Yang et al., 2021). Therefore, in carsharing systems, especially in one-way carsharing systems, it is necessary to relocate vehicles between stations to meet users' travel demands. Moreover, staff are employed to relocate vehicles between stations which means that their movements during the day cannot be ignored for overall system efficiency maximization (Santos and Correia, 2019). In the one-way carsharing system, there are two subtypes of systems: free-floating and station-based. The users are allowed to book the vehicles at any location within a specified area in free-floating systems, while in station-based systems, the user must pick up and return the shared car at a designated parking station. In this paper, we focus on station-based systems, although the methods that are going to be proposed could eventually be easily extended to a free-floating system. Notably, each staff is usually equipped with a folding bicycle or an electric scooter to move between the relocation tasks (Bruglieri et al., 2014; Bruglieri et al., 2017; Bruglieri et al., 2018). The process of vehicle relocation in the station-based carsharing system can be briefly described as follows. When receiving the relocation tasks, the staff departs from one station (or depot) to the station where a shared car needs to be relocated using a folding bicycle or an electric scooter. Thereafter, the staff places the folding bicycle or the electric scooter in the shared car and drives the shared car to a target station to complete the relocation task. The staff then uses the folding bicycle or the electric scooter to move to the next station for another relocation task or return to the depot. Carsharing companies with more shared cars require fewer relocation operations between stations and therefore require fewer staff members (Weikl and Bogenberger, 2013; Nourinejad et al., 2015). However, the high cost of buying the shared vehicles and paying for the stations' space usage limits the fleets that can be bought (Jorge et al., 2014). As the vehicles are relocated by staff, an imbalance of the relocation staff can also occur. Hence, relocations in carsharing systems involve both vehicle relocation and staff rebalancing operations.

The users reserve shared cars via a mobile app and then pick them up at a specific location. They need to register as members and pay the registration fee in advance before the reservation process. Shared cars are usually billed by time, but some companies also use the "minute plus mileage" method. In station-based systems, each company sets up specific stations where users can pick up the shared cars. The shared cars from one company are not allowed to return to other companies' stations, and each company employs staff to perform the relocation operations among its own stations. The boom of multiple carsharing companies in the city offers convenience to users. For example, the competition between companies may make carsharing trips less expensive. They also provide more vehicles and parking stations for users to choose from. However, because of the high registration fees, most users only choose one suitable carsharing company based on their travel needs, which restricts them to only using the shared cars of the companies that they have registered with.

Carsharing companies are growing, yet they face a variety of problems (Sohu News, 2017). A single carsharing company often cannot purchase a large number of shared cars and set up many stations because of the high cost of buying and equipping vehicles, together with the cost of parking, maintenance, gas, and insurance for the vehicles. Too few vehicles or too few stations, and a mismatch between the number of vehicles and parking spaces can lead to a loss of customers. In addition, the tidal phenomenon of users' travel demands has typically caused an imbalance in vehicle inventory, resulting in a shortage of vehicles at some stations, while others lack parking spaces. Therefore, carsharing companies need to employ sufficient staff to perform the relocation tasks. As travel demand varies significantly among different stations at different periods of the day, the staff will be busy during peak hours and idle during non-peak hours. Currently, most of the carsharing companies work separately in cities. Without effective relocation operations and cooperative strategies, the utilization rate of the shared vehicles may be lower than what could eventually be achieved if cooperation takes place. Owing to the blind expansion of carsharing companies, many of them have closed down and announced their withdrawal from the market.

Accurate carsharing travel demand prediction helps the system pre-arrange the relocation routes to satisfy the dynamic needs of different stations (Santos and Correia, 2019; Huo et al., 2020). However, carsharing travel demand prediction is dependent on the complex spatio-temporal relationships among stations and the external environmental factors such as the weather and land-use characteristics, which make the task challenging. In recent years, deep learning based data modeling algorithms have been supported by scholars for their powerful ability to learn the correlated feature representations (Ke et al., 2021). For the carsharing travel demand prediction tasks, existing studies usually use the long short-term memory (LSTM) neural network (Yu et al., 2020) and gated recurrent unit (GRU) (Vateekul et al., 2021) to capture the temporal characteristics. Although LSTM and GRU structures can adequately extract temporal dependencies from the historical data, they fail to effectively model the spatial relations. In carsharing

systems, the stations are nodes in a network topology. The convolutional neural network (CNN) can extract the spatial dependence of the data with a grid-like structure. However, this fails to reflect the non-Euclidean structures. Graph convolutional network (GCN) is designed to model the complex topological structure of the relations between objects which fit carsharing station networks. Multi-step carsharing demand forecasts provide not only a prediction of the system state in the next time step but also information about long-term trends, which is more beneficial for relocation route planning.

In this study, we present a data-driven, dynamic, and cooperative method for vehicle relocation and staff rebalancing in carsharing systems in the context of multiple carsharing companies operating in the same city. The main contributions of this study are highlighted as follows:

- We propose a novel attention-enhanced temporal graph convolutional network (AE-TGCN) model for multi-step flow prediction in carsharing systems, which integrates the GCN layer, GRU layer, and the attention mechanism to extract the features from temporal and spatial variables collaboratively.
- We establish a two-phase integer programming model to optimize the process of vehicle relocation and staff rebalancing.
- The cooperative relocation strategies, including the sharing of relocation staff and the sharing of vehicles and stations among the different companies are proposed to increase the utilization rate of shared vehicles and relocation staff members.
- We adopt a rolling horizon approach to work with real-time relocation demand. The Adaptive Large Neighborhood Search (ALNS) based heuristic approach is implemented to solve the model.
- The effectiveness of our proposed model and cooperative relocation strategies are assessed based on the 6-month real-world travel records from four carsharing companies in the city of Fuzhou, China.

The remainder of this paper is organized as follows. A review of the literature on demand forecasting and vehicle relocation in carsharing systems is provided in Section 2. In Section 3, we describe the entire framework and the methodology. Section 4 elaborates on the ALNS based heuristic solution method. Section 5 analyzes the spatiotemporal travel patterns of shared cars using real-world data in the city of Fuzhou, China. In Section 6, we apply the methodology to the case study city and analyze the main results. Finally, the conclusions are summarized in Section 7.

2. Literature review

2.1. Demand prediction in carsharing systems

The travel demand for carsharing trips is influenced by many factors. To understand what factors affect the users' behavior when selecting vehicles in the carsharing system, Jian et al. (2016a) proposed a spatial hazard-based model that investigates the users' socio-demographic attributes, vehicle characteristics, and land use type of the trip origin on choice set formation. Jian et al. (2017) analyzed users' vehicle choice behavior and utilization patterns in a carsharing system with the multiple discrete–continuous extreme value model. The results suggest that user age, income level, driving license country, insurance plan, membership plan, and origin location impact users' vehicle utilization patterns. Jorge and Correia (2013) reviewed the advanced methods to study the demand estimation and planning issues of carsharing systems, suggesting that a significant effort must be made to develop more general and realistic models to accurately represent the characteristics of carsharing and apply them to solve one-way carsharing problems. Schmöller et al. (2015) studied the free-floating carsharing usage patterns and identified the factors that influence the demand. The temporal carsharing demand shows recurring patterns while high demand occurs on a few temporal peak hours. The spatial travel demand is concentrated on some hot spots correlated with the area functions. In addition, some external influences such as weather conditions and precipitation affect the usage of shared cars. For example, the travel demand is approximately 6% higher than the average on rainy days. In addition, carsharing usage depends on the user's activity patterns, while these patterns are essentially changing (Kek et al., 2009; Hu et al., 2019). In residential areas, shared cars may be in short supply during morning peak hours, because more people use shared cars to commute during that time, whilst in commercial areas, shared cars may face parking space shortages.

Accurate prediction of travel demand for carsharing is a prerequisite for successfully identifying the spatio-temporal imbalance among stations. An accurate flow prediction model helps system operators pre-allocate the cars to meet the user's travel demand. Becker et al. (2017) modeled the carsharing use in Switzerland using spatial regression and conditional logit analysis. The results show that shared cars are usually used for discretionary trips and bridge gaps in the existing public transportation networks. Wang et al. (2020a) used multi-source data, including real-time user application log data, order data, and user characteristics to predict the real-time pickup demand with a multivariate linear regression model. According to the results, the dynamic demand prediction model can effectively guide the system to optimize vehicle relocation, which not only increases the profit of the carsharing system but also improves the quality of the service.

Machine learning algorithms such as support vector regression (SVR) and ensemble decision trees, can handle large volumes of data and learn complex relationships for travel demand prediction. Boldrini et al. (2019) forecasted the carsharing demand in ten European cities with random forest (RF) and neural network (NN). The results show that more accurate predictions are obtained using machine learning methods compared with statistical models. Wang et al. (2020b) employed the gradient boosting regression trees (GBRT) model to predict station-level carsharing usage. The results indicate that the GBRT model predicts users' travel demands with high accuracy, and time-varying variables are imperative for the prediction of carsharing usage.

Despite the cited studies, employing deep learning methods for demand forecasting in one-way carsharing systems is still limited in capturing both spatial and temporal relations effectively. Zhang et al. (2019) modeled the hourly variation in carsharing systems

Table 1
Studies on the operator-based carsharing relocation problem in the literature.

References	Relocation demand	Staff rebalancing	Cooperative strategy	Approach	Objective	Solution method
Nourinejad et al. (2014)	Given	No	No	Binary integer programming	Maximize the total profit of the system	Branch and cut algorithm
Jorge et al. (2014)	Given in a simulation model	No	No	MIP	Maximize the profitability of a carsharing service	Branch and cut algorithm
Weikl and Bogenberger (2015)	Predicted	No	No	MIP	Maximize the profit resulting from vehicle movements between zones.	Branch and cut algorithm
Nourinejad et al. (2015)	Given	Yes	No	MIP	Minimize the total cost, including the cost of vehicle relocation and staff rebalance	A heuristic with a decomposition method
Boyacı et al. (2015)	Given	No	No	Multi-objective MIP	Maximize the net revenue for the operator and the users' net benefit	Branch and bound algorithm
Bruglieri et al. (2017)	Given	Yes	No	MILP	Maximize the total profit between the revenue of the satisfied relocation requests and the cost of all the workers used	A ruin and recreate metaheuristic
Boyacı et al. (2017)	Given	Yes	No	Multi-objective MIP	Maximize the number of trips served and minimize relocation cost	Clustering algorithm and branchand-cut algorithm
Bruglieri et al. (2018)	Given	Yes	No	Multi-objective MILP	Minimize the total number of workers employed; Maximization the customers' satisfaction; Minimize the duration of the longest route	A two-phase heuristic algorithm
Zhao et al. (2018)	Given	Yes	No	MILP; space–time network	Minimize the total cost, including the vehicle and staff investment, and operation expenses.	Lagrangian relaxation-based solution approach
Gambella et al. (2018)	Given	Yes	No	MIP; rolling horizon	Maximize the profit associated with the trips performed by users	A model-based heuristics with removing relocation and rolling horizon approach
Xu and Meng (2019)	Randomly generated	No	No	Set partitioning model	Maximize the profit of a carsharing operator	A tailored branch-and-price approach
Repoux et al. (2019)	Predicted by Markov chain	No	No	Rolling horizon optimization framework	Maximize the number of accepted requests	Solved iteratively via a rolling horizon framework
Santos and Correia (2019)	Forecasted using a homogeneous Poisson process	Yes	No	MIP; rolling horizon	Minimize the generalized cost, including the cost of the vehicle and staff relocation, the potential profit losses, and a penalty for maintenance requests not executed.	Branch and cut algorithm
Huo et al. (2020)	Following the Poisson distribution	No	No	Data-driven optimization model; linear programming	Maximize the overall profit, including the expected income and dispatching cost	Branch and cut algorithm
Folkestad et al. (2020)	Given	Yes	No	MIP	Minimize the cost of relocating and the costs of postponed charging.	Hybrid genetic search with adaptive diversity control algorithm
Yang et al. (2021)	Given	Yes	No	Integer linear programming; rolling horizon	Minimize the generalized daily operational cost	A customized decomposition algorithm.
This study	**Predicted by AE-TGCN**	**Yes**	**Yes**	**Integer linear programming; rolling horizon**	**Maximize the overall profit, including the expected income, vehicle relocation cost, and staff rebalancing cost**	**An adaptive large neighborhood search based heuristic approach**

including travel demand and travel distance based on the long short term memory recurrent neural network (LSTM-RNN). The results show a greater performance compared with the SVR and classic autoregressive integrated moving average (ARIMA) model. Yu et al. (2020) established an LSTM network structure for forecasting vehicle pick-up and drop-off over time in a station-based carsharing system, where the model captures multiple temporal features, including day of week, time of day, and weather conditions. Vateekul et al. (2021) used a bidirectional GRU to forecast the real demand in the carsharing system. These time-series modeling methods are often applied to predict the travel demand of a single station separately, ignoring the spatial relations among stations. To effectively capture the complex spatial relations, Zhu et al. (2019) proposed a multi-graph convolutional model, where the spatial distance characteristics and land use characteristics are extracted using the GCN. Therefore, new methods should be explored to simultaneously capture complex spatial relations and temporal dynamics, which can integrate not only historical travel demand characteristics but also the influence of external factors such as weather events.

2.2. Vehicle relocations in carsharing systems

Jorge and Correia (2013) identified vehicle relocations as an effective strategy for reducing the cost of one-way carsharing systems, which can be implemented with the user-based approach and the operator-based approach. User-based relocation is performed by the customer to modify their trips to help the system restore a balanced distribution of vehicles through various incentive mechanisms. Febbraro et al. (2019) established a user-based relocation method for maximizing the profit in carsharing systems, where the users are allowed to leave the car at different locations in exchange for fare discounts. The results show that the number of rejected reservations is reduced and the operator's profit can be increased with the proposed strategy. Schiffer et al. (2021) adopted user-based relocation to increase the utilization rate in free-floating carsharing systems. They reformulated the problem as a k-disjoint shortest path problem and proposed an exact algorithm to solve large-size examples. Wang et al. (2021) developed a user-based multi-objective relocation model with the objectives of profit maximization and using failure rate minimization. User-based relocation techniques shift the burden of relocating vehicles to the users, which alleviates the relocation tasks of staff. However, most travelers care more about privacy and convenience instead of obtaining minor transport cost savings, especially during peak hours. With the operator-based approach, carsharing companies employ staff to relocate the vehicles from one station to another. Along with the vehicle relocation operations, there is an imbalance of staff. Therefore, staff should move between stations to perform vehicle relocation operations (Nourinejad et al. 2015; Yang et al., 2021). We summarize the scientific literature on operator-based carsharing relocations in Table 1 according to the relocation demand determination, modeling approach, objectives, solution algorithms, and whether staff rebalancing and collaborative relocation are considered or not.

Simulation and mixed-integer programming (MIP) approaches are widely used for planning and managing operator-based vehicle relocation tasks (Illgen and Hoeck, 2019). Weikl and Bogenberger (2013) proposed a two-step relocation model for carsharing systems, which consists of an offline demand clustering that allows for the demand prediction, and the online optimal vehicle reposition. Nourinejad et al. (2014) proposed a dynamic vehicle relocation model to reduce the vehicle imbalance in one-way carsharing systems, which maximizes the total profit by considering the generated revenue and the cost of relocation. They concluded that the dynamic model was more practical and can build robust route decisions. Jorge et al. (2014) established a mathematical programming model to optimize the relocation operations that maximize the profit of a one-way carsharing company. A simulation model was combined to study different real-time relocation policies. Jian et al. (2016b) studied the dynamic vehicle relocation in a carsharing system for both one-way and round-trip services. They proposed an optimization model to determine the relocation routes by maximizing the profit for carshare operators. The results based on the real-world trip demand data indicate that the maximum profit occurs when the price of a one-way trip is approximately four times higher than that of a round trip. Xu and Meng (2019) formulated a set partitioning model to determine the vehicle fleet size for one-way carsharing services with an electric fleet. The proposed model is designed to maximize the profit of a carsharing operator, which considers the vehicle relocation operations and electric vehicle charging profiles. Carsharing travel demand is influenced by the supply of vehicles, and the demand further changes the vehicle availability in the system. Focusing on this problem, Jian et al. (2019) proposed an integrated supply–demand approach to solve the vehicle relocation in a carsharing system, where a discrete choice model is incorporated within the optimization formulation. Huo et al. (2020) proposed a data-driven relocation model that considers the demand uncertainty of an electric carsharing system. They adopted discrete stochastic probabilities to express order uncertainty and used a rolling horizon approach to dynamically update the data. Wu et al. (2021) designed an integer linear programming model to address the joint design problem of carsharing systems, where all-day vehicle relocation and dynamic trip selection are considered. The results illustrate that the relocation operation plays an essential role in both profit maximization and demand satisfaction. Considering the demand uncertainty in the carsharing system, Huang et al. (2021) studied the demand–supply imbalance problem by combining a long-term pricing strategy and real-time vehicle relocations in a two-stage stochastic programming model. The application in Suzhou, China shows that adjusting the price of carsharing is effective in the long-term imbalance problem. Although the above studies have shown impressive results to solve the imbalance problem in the carsharing system, some studies assume that the staff is enough to do relocations and overlook the rebalancing of the relocation staff that determines how the staff should perform different vehicle relocation tasks. Besides, the relocation demand or user requests are often assumed to be known in advance. For example, Huo et al. (2020) assumed that the pick-ups and arrivals in each station follow a Poisson distribution.

To jointly optimize the vehicle relocation and staff rebalancing process, Bruglieri et al. (2014) proposed the first Mixed Integer Linear Programming (MILP) formulation to restore a better distribution of the vehicles by workers in a one-way electric carsharing system. The performance of the MILP formulation was tested on instances built on the Milan road network. The economic sustainability of vehicle relocation was considered in Bruglieri et al. (2017), where a MILP formulation for the electric vehicle relocation problem was proposed with operators using folding bicycles to facilitate vehicle relocation. The model aimed to maximize the total

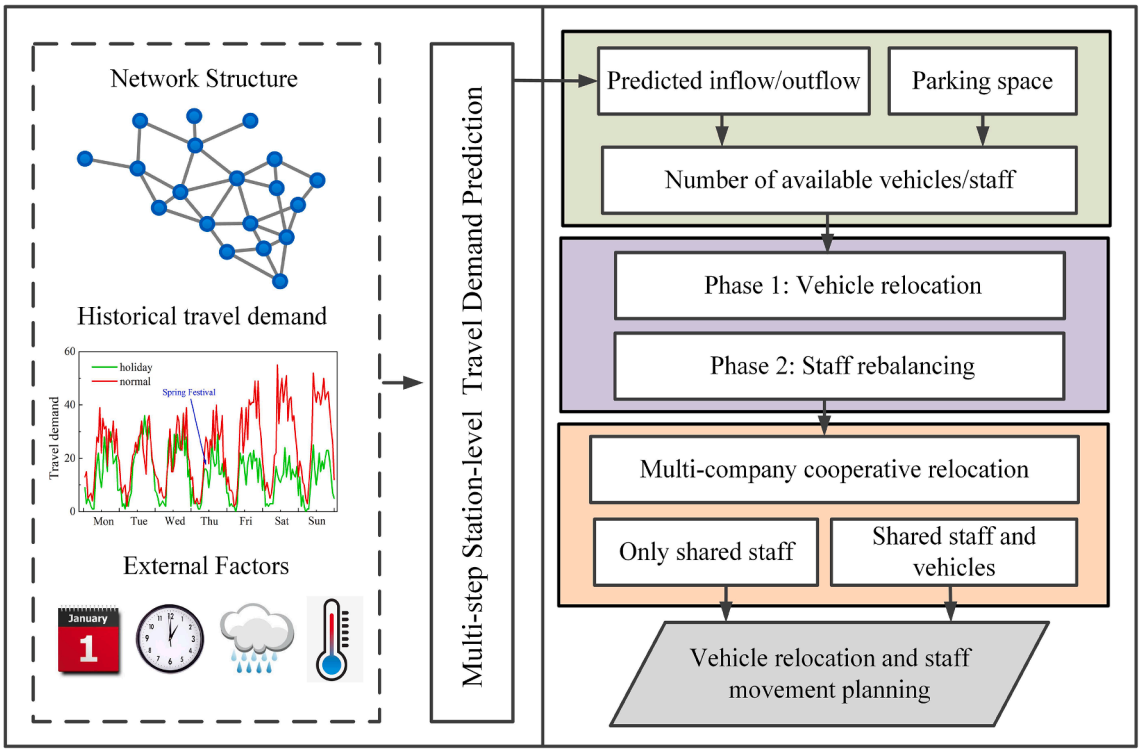

Fig. 1. An overview of the multi-company cooperative relocation framework.

profit between the revenue of the satisfied relocation requests and the cost of all the workers used. In addition, a ruin and recreate metaheuristic was designed to find better solutions within a shorter computational time. Bruglieri et al. (2018) adopted a two-phase optimization method for the multi-objective vehicle relocation problem that considers the minimization of the total number of workers employed, the maximization of customer satisfaction, and the minimization of the duration of the longest route. The proposed method not only reduced relocation costs and increased the service level, but also provided a fair distribution of the relocation requests among workers. Zhao et al. (2018) modeled the dispatching routes of shared electric vehicles and staff using a space–time network and formulated them into a MILP model. A Lagrangian relaxation-based solution approach was developed to solve this model more efficiently and accurately. Santos and Correia (2019) formulated the vehicle relocation and staff rebalancing problem in a MIP model, where the staff are rebalanced between zones with public transport. Based on the rolling-horizon approach, the activities of the staff including vehicle relocation and maintenance were planned to satisfy the real-time demand. Huang et al. (2020) compared the efficiencies of the operator-based and user-based relocation station-based electric carsharing systems. The optimization results show that both two methods can effectively alleviate the imbalance problem. Yang et al. (2021) adopted a time–space network approach to represent the double-balanced dynamic optimization of both vehicle relocation and staff scheduling. An integrated model was proposed to minimize the generalized daily operational cost, and two different time granularities were designed to obtain the optimized relocation tasks and the refined scheduling of the relocation staff. To avoid the imbalance of available vehicles at different car-sharing stations, Lu et al. (2021) focused on the vehicle relocation problem with operation teams. In contrast to previous relocation modes where workers ride a folding bicycle to travel between stations, the company uses operation teams to perform relocations.

Cooperative strategies are used when two or more companies want to partner and work together to achieve common objectives. Cooperative planning has been applied to truck scheduling and planning in a seaport environment. Typically, a truck must return to the pick-up point after picking up or delivering a full container in a port. In this case, it does an empty move, which loses the carrier's profit and may incur a surged congestion on roads as well. Caballini et al. (2016) proposed an optimization model for the cooperative planning of multiple truck carrier operations that serve the hinterland area of a port. They properly organized the trips belonging to the same carrier and introduced cooperative strategies to allow different carriers to share their needs and find the most suitable trip combination in a broader context. This ensures an increased profit in the real daily truck trip operations with respect to that without collaboration. Phan and Kim (2016) proposed an iterative collaborative model through which different truck companies and terminals can collaborate to determine more suitable truck schedules. The results show that the collaborative process can minimize the truck travel cost and truck waiting time under practical operating conditions.

Previous studies have presented several breakthroughs and innovations in the methods for solving the carsharing relocation problem. However, there is still much to be investigated. (i) The relocation demand or user requests are most of the times assumed to be known in advance. New forecasting algorithms in deep learning can capture the fluctuating spatiotemporal characteristics of travel demand and better predict the future states of the stations, which play a vital role in dynamically relocating the shared cars. (ii) Some

models in the literature assume that the staff is sufficient to relocate the vehicles. In practice, the available staff is limited and varies throughout the day, which should be better scheduled to perform the vehicle relocation tasks between stations. (iii) Previous studies have focused on carsharing relocations in a single carsharing company, without considering multi-company cooperation. Based on the current status of multi-company carsharing operations, timely vehicle relocation and staff rebalancing, as well as effective cooperation strategies, may provide new solutions to the problems of the low utilization rate of vehicles in current carsharing companies.

3. Methodology

In this study, we propose a data-driven, dynamic, and cooperative method for vehicle relocation and staff rebalancing in one-way carsharing systems. The entire framework includes a multi-step travel demand prediction, vehicle relocation and staff rebalancing optimization, and multi-company collaboration in shared resources (see Fig. 1). The framework starts with the prediction of the number of shared cars at each station and ends with the vehicle relocation route and staff movement planning. The rolling-horizon approach is applied to dynamically plan the relocation activities, which allows the system to adapt to real-time demand.

3.1. Multi-step travel demand prediction model

In this section, we propose an attention-enhanced temporal graph convolutional network (AE-TGCN) model for multi-step flow prediction in a carsharing system. The undirected graph $\mathscr{G} = (I, E)$ is used to construct the topology of the carsharing network. We consider each station as a node in the network, where $I = \{1, 2, \cdots, N\}$ is the set of stations, and E is the set of edges representing the relation between two stations. The historical travel demand is regarded as the attribute of nodes in the network, $X \in \mathbb{R}^{N\times P}$, where N is the number of stations in the carsharing network and P is the length of the historical time series. In addition, the external attributes such as static land-use characteristics L and dynamic weather conditions W can be flexibly fused to build the feature matrix, $\mathscr{T}_t = [X_t, W_t, L]$. Therefore, the multi-step travel demand prediction problem at shared car stations is to learn a function f that can map travel demand in the previous P time steps to that in the next $\mathscr{T}$ time steps based on carsharing network topology G and the feature matrix $\mathscr{T}$, in Eq. (1).

$$[X_{t+1}, \cdots, X_{t+\mathscr{T}}] = f(G; [\mathscr{T}_{t-P}, .., \mathscr{T}_t]) \tag{1}$$

3.1.1. Spatial feature modeling

The graph convolutional network (GCN) is used to capture the spatial relations among stations (Lin et al., 2018; Zhao et al., 2019). The connections between stations are described in a carsharing network by defining an adjacency matrix, $\mathscr{A} \in \mathbb{R}^{N\times N}$. Given the adjacency matrix $\mathscr{A}$ and the feature matrix $\mathscr{T}_t$ defined above, the GCN constructs a filter in the Fourier domain. The modeling process is represented in Eq. (2).

$$H^{(l+1)} = \sigma\left(\widetilde{D}^{-\frac{1}{2}}\widetilde{\mathscr{A}}\widetilde{D}^{-\frac{1}{2}}H^{(l)}\theta^{(l)}\right) \tag{2}$$

where $\widetilde{\mathscr{A}} = \mathscr{A} + I_N$ is the adjacency matrix including self-connections, and I_N is the unit matrix. $\widetilde{D}$ is the degree matrix of the carsharing network, $\widetilde{D} = \sum_j \widetilde{\mathscr{A}}_{ij}$. $\theta^{(l)}$ is the training parameter of the *l-th* layer. $\sigma(\cdot)$ denotes the ReLU activation function.$H^{(l)}$ is the output of the *l-th* layer.

For example, given the feature matrix $\mathscr{T}_t$ and the adjacency matrix $\mathscr{A}$, a 2-layer GCN model can be expressed as in Eq. (3).

$$g(\mathscr{T}_t, \mathscr{A}) = \sigma\left(\widehat{\mathscr{A}}\sigma\left(\widehat{\mathscr{A}}\mathscr{T}_t\theta^{(1)}\right)\theta^{(2)}\right), \widehat{\mathscr{A}} = \widetilde{D}^{-\frac{1}{2}}\widetilde{\mathscr{A}}\widetilde{D}^{-\frac{1}{2}} \tag{3}$$

where $\theta^{(1)}$ is the trainable weight matrix from the input layer to the hidden layer and $\theta^{(2)}$ is the trainable weight matrix from the hidden layer to the output layer. $g(\mathscr{T}_t, \mathscr{A}) \in \mathbb{R}^{N\times\mathscr{T}}$ represents the predicted carsharing demand for the next $\mathscr{T}$ time steps.

In this study, we define the adjacency matrix $\mathscr{A}$ to quantify the relationship between stations based on the travel demand in Eq. (4).

$$\mathscr{D}_{ij}^{'} = \begin{cases} \mathscr{D}_{ij} + \mathscr{D}_{ji} & if\ i \neq j \\ \mathscr{D}_{ij} & otherwise \end{cases} \tag{4}$$

where $\mathscr{D}_{ij}$ is the travel demand from station i to station j. If the daily travel demand $\mathscr{D}_{ij}^{'}$ is higher than a predefined threshold, we suppose that the two stations are connected with $\widetilde{\mathscr{A}}_{ij} = 1$ otherwise $\widetilde{\mathscr{A}}_{ij} = 0$. Shared cars from different companies can only be picked up and parked at the corresponding stations. Therefore, if two stations belong to two different companies, they will not be connected in the graph representation of the carsharing network.

3.1.2. Temporal feature modeling

The inflow and outflow travel demands at the carsharing stations are strongly time-dependent. In deep learning theory, Recurrent Neural Network (RNN) is developed for time series data modeling, which takes historical information from prior inputs to influence the current input and output. However, the problems of vanishing gradient and exploding gradient exist with the long-sequence input. Gated recurrent unit (GRU) (Vateekul et al., 2021) network introduces memory cells to learn whether the previous hidden layer state

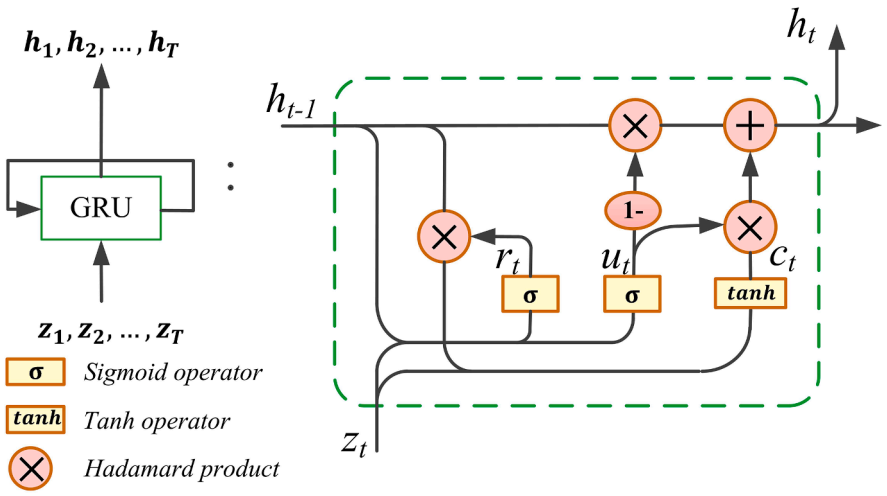

Fig. 2. Structure of GRU network.

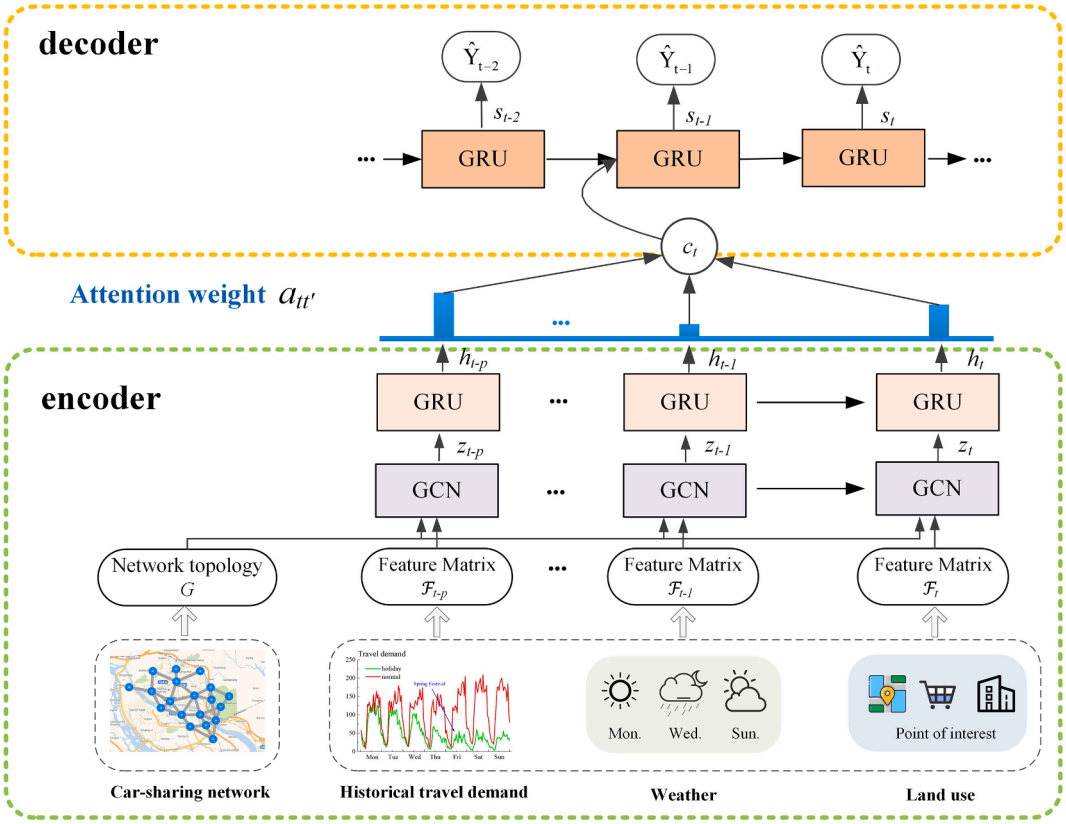

Fig. 3. The structure of the AE-TGCN model.

needs to be forgotten or updated, which can control the information to be memorized with a shorter training time. The structure of the GRU network is shown in Fig. 2.

In Eq. (5), the GCN outputs the station-level travel demand predictions in a vector z_t with the mapping function $g(\cdot)$, which is the input of the GRU.

$$z_t = g(\mathscr{F}_t, \mathscr{A}) \tag{5}$$

Update gate:

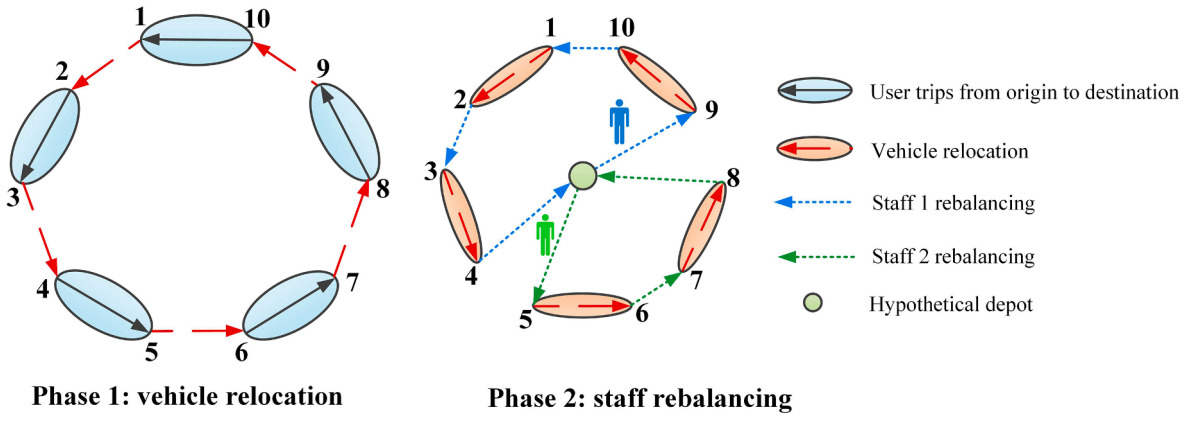

Fig. 4. Illustration of vehicle relocation and staff rebalancing.

$$u_t = \sigma(W_u * [z_t, h_{t-1}] + b_u) \tag{6}$$

Reset gate:

$$r_t = \sigma(W_r * [z_t, h_{t-1}] + b_r) \tag{7}$$

Cell state:

$$c_t = tanh\left(W_c[z_t, (r_t * h_{t-1})] + b_c\right) \tag{8}$$

Output state:

$$h_t = u_t * h_{t-1} + (1 - u_t) * c_t \tag{9}$$

In Eq. (6)–(8), u_t, r_t, and c_t are the update gate, reset gate, and memory cell state at time t. W_u, W_r, and W_c are the corresponding weight update matrices; b_u, b_r, and b_c are the corresponding bias vectors. The update gate u_t controls the state information at the previous time, which should be brought into the current state. The reset gate r_t controls the degree to which the state information is ignored at the previous moment. The cell state c_t combines the information at the previous moment and current memory to calculate the output state h_t, which captures the temporal variation trends of the carsharing travel demand.

3.1.3. The attention mechanism

The encoder-decoder architecture provides a standard approach using deep neural networks to deal with sequence-to-sequence prediction problems (Duan et al., 2021). In the traditional encoder-decoder architecture, the first process encodes the features into a fixed-length vector, and the second process decodes the fixed-length vector to obtain the multi-step outputs (Chang et al., 2021). However, the fixed-sized vector generated by the encoder fails to model long inputs (Hao et al., 2019). Therefore, in this study, we employ an attention mechanism to enhance the internal representation of the spatial and temporal characteristics of the carsharing network in a context vector c_t, as shown in Fig. 3.

When making the predictions for output $\{X_{t+1}, \cdots, X_{t+\mathscr{T}}\}$, the attention score $a_{tt'}$ $(t' = t - P, \cdots, t)$ specifies the amount of attention that the encoder hidden state $\{h_{t-P}, \cdots, h_t\}$ should be paid to the decoder to make predictions at time t in Eq. (10).

$$c_t = \sum_{t'=1}^{P} a_{tt'} h_{t'} \tag{10}$$

$$a_{tt'} = \frac{exp(e_{tt'})}{\sum_{t'=1}^{P} exp(e_{tt'})} \tag{11}$$

$$e_{tt'} = \zeta(s_{t-1}, h_{t'}) \tag{12}$$

The attention score $a_{tt'}$ is calculated by an alignment model in Eq. (11). ζ in Eq. (12) represents an operation of a fully connected feed-forward neural network to generate the scores of each time step state in the encoder network (Hao et al., 2019).

The entire framework of the AE-TGCN model is shown in Fig. 3. The encoder-decoder architecture allows the model to predict the value of inflow and outflow of all carsharing stations in future time steps, termed as multi-step flow prediction. The loss function of the AE-TGCN model is given by Eq. (13). The first term is used to minimize the error between the actual travel demand Y_i and the predicted value $\widehat{Y}_i$. n is the size of the sample set. The second term L_{reg} is the L_2 regularization term that helps avoid overfitting and λ is a hyperparameter (Zhao et al., 2019).

Table 2
Notations in the vehicle relocation optimization model.

Parameters	
V	set of space–time vertices in the space–time network
A	set of space–time arcs in the space–time network
T	set of time intervals
k	index for carsharing company,$k = 1, 2, ..., K$
I_k	set of parking stations of company k
i_k, j_k	indexes of carsharing parking stations of company k, $i_k, j_k \in I_k$
t, s	indexes of different time intervals,$t, s \in T$
$(i_k, t), (j_k, s)$	indexes of space–time vertices,$(i_k, t), (j_k, s) \in V$
(i_k, t, j_k, s)	index of space–time arc, $(i_k, t, j_k, s) \in A$
$d_{(i_k,t)}$	the predicted departure demand of station i_k at time interval t in number of customers
$f_{(i_k,t)}$	the predicted arrival demand of station i_k at time interval t in number of customers
ps_{i_k}	number of parking spaces available at station i_k
$w_{(i_k,t)}$	average rental revenue per order for station i_k at time interval t
$s_{i_k j_k}$	minimum travel distance between station i_k and j_k
α	the vehicle relocation cost per kilometer
β	the penalty cost for not fulfilling or delaying one user's request
Auxiliary variables	
$ic_{(i_k,t)}$	the revenue of the station i_k at time interval t when the number of user demand is $x_{(i_k,t)}$
$cr_{(i_k,t)}$	the dispatching distance cost of station i_k at time interval t
$cp_{(i_k,t)}$	the penalty cost for not fulfilling customers' requests at station i_k at time interval t
Decision variables	
$x_{(i_k,t)}$	the number of vehicles departing with customers at station i_k at time interval t
$o_{(i_k,t)}$	the number of vehicles available at station i_k at time interval t
$z_{(i_k,t,j_k,s)}$	the number of vehicles moving from station i_k at time interval t to station j_k at time interval s

$$loss = \sum_{i=1}^{n} |Y_i - \widehat{Y}_i| + \lambda L_{reg} \tag{13}$$

3.2. Two-phase vehicle relocation and staff rebalancing model

The relocation of shared cars can lead to an imbalance of staff in a city. Therefore, relocation operations in one-way carsharing systems should address both the optimization of the vehicle relocation and the staff rebalancing. The system continuously updates the number of shared cars and staff activities at the stations to ensure that users' travel needs are satisfied throughout the day.

In this study, we use a space–time network to integrate physical carsharing networks with the time-dependent movements and activities of both vehicles and staff. The working time during the day is divided into M time periods of duration δ. Thereafter the set of time intervals can be expressed as $T = \{t_0, t_0 + \delta, \cdots, t_0 + M\delta\}$. The set of shared car stations is $I = \{1, 2, \cdots, N\}$. The set $V = \{1_{t_0}, 1_{t_0+\delta}, \cdots, N_{t_0+M\delta}\}$ denotes the time–space network constituted by all the $N \times M$ vertices. The set of arcs between the vertices defined in V is designated as A. Fig. 4 illustrates the process of optimal vehicle relocation (Phase 1) and the staff rebalancing process (Phase 2) for 10 carsharing stations. Five user trips (e.g., the arc between 2 and 3, the arc between 4 and 5, etc.) and vehicle relocation trips (e.g., the arc between 1 and 2, the arc between 3 and 4, etc.) are represented in Phase 1. Two shared vehicles are relocated by the two staff to serve five customer trips in Phase 2.

3.2.1. Phase 1: Vehicle relocation optimization

Phase 1 is a vehicle relocation optimization model based on the predicted inflow/outflow travel demand in a multi-company carsharing system. To solve this problem, the notations are presented in Table 2.

The objective function of the problem is:

$$Maximize(\Pi_1) = \sum_{k \in K} \sum_{(i_k,t) \in V} \left(ic_{(i_k,t)} - cr_{(i_k,t)} - cp_{(i_k,t)} \right) \tag{14}$$

Subject to:

$$ic_{(i_k,t)} = w_{(i_k,t)} \cdot x_{(i_k,t)}, \ \forall (i_k, t) \in V \tag{15}$$

$$cr_{(i_k,t)} = \sum_{j_k \in I_k} \alpha \cdot s_{i_k j_k} \cdot z_{(i_k,t,j_k,s)}, \forall i_k \in I_k, (i_k, t, j_k, s) \in A \tag{16}$$

$$cp_{(i_k,t)} = \beta \cdot \left(d_{(i_k,t)} - x_{(i_k,t)} \right), \ \forall (i_k, t) \in V \tag{17}$$

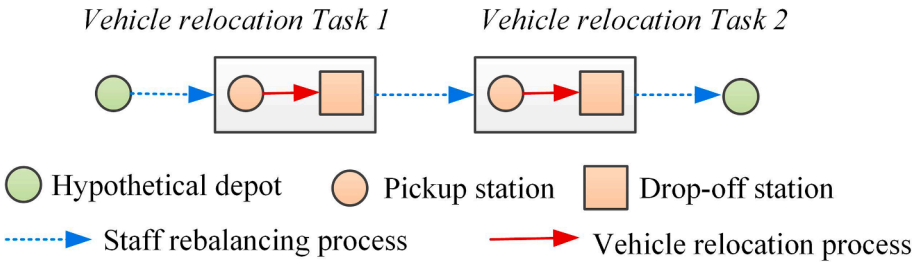

Fig. 5. Illustration of the staff rebalancing process.

$$o_{(i_k,t)} = o_{(i_k,t-1)} + \sum_{(j_k,s,i_k,t)\in A} z_{(j_k,s,i_k,t)} - \sum_{(i_k,t,j_k,s)\in A} z_{(i_k,t,j_k,s)} + f_{(i_k,t)} - x_{(i_k,t)},\ \forall (i_k,t) \in V \tag{18}$$

$$0 \le o_{(i_k,t)} \le ps_{i_k}, \forall i_k \in I_k, t \in T \tag{19}$$

$$x_{(i_k,t)} \le o_{(i_k,t-1)} + f_{(i_k,t)} + \sum_{(j_k,s,i_k,t)\in A} z_{(j_k,s,i_k,t)},\ \forall (i_k,t) \in V \tag{20}$$

$$x_{(i_k,t)} \le d_{(i_k,t)},\ \forall (i_k,t) \in V \tag{21}$$

$$z_{(i_k,t,j_k,s)} \in \mathbb{N}, \forall (i_k,t,j_k,s) \in A \tag{22}$$

$$x_{(i_k,t)}, o_{(i_k,t)} \in \mathbb{N},\ \forall (i_k,t) \in V \tag{23}$$

The objective function (14) maximizes the profit of the multi-company carsharing system, which includes:

- Expected revenue $ic_{(i_k,t)}$. The calculation of the expected income of station i_k considers the number of satisfying users' demand $x_{(i_k,t)}$ and the average rental revenue $w_{(i_k,t)}$ in constraints (15). $w_{(i_k,t)}$ is the average rental revenue per order for station i_k at time interval t. Here we consider that the average rental income is changed at different time intervals, and we use the historical average method to calculate $w_{(i_k,t)}$.
- Vehicle relocation cost $cr_{(i_k,t)}$. The vehicle relocation cost of Phase 1 is determined by the number of vehicles to be relocated from the station i_k, the distance traveled, $s_{i_k j_k}$, and the unit relocation cost α, as shown in constraints (16).
- Penalty cost for not fulfilling the customers' travel demands $cp_{(i_k,t)}$. The unmet customer demand for station i_k at time interval t is $d_{(i_k,t)} - x_{(i_k,t)}$ in constraints (17), and β is the unit penalty cost for not fulfilling a customer travel demand.

Constraints (18) update the number of vehicles available at station i_k at the beginning of time interval t, considering the shared vehicles used by customers and relocated by staff. Constraints (19) are the parking capacity constraints to ensure that the number of available vehicles at station i_k should not exceed the number of parking spaces ps_{i_k}. Constraints (20) set the upper bound of the number of shared vehicles that users can pick up from station i_k. Constraints (21) ensure that the met demand does not exceed the predicted actual demand. Constraints (22) and (23) set the domains of the variables $z_{(i_k,t,j_k,s)}$, $x_{(i_k,t)}$ and $o_{(i_k,t)}$.

After solving the vehicle relocation optimization problem, the relocation tasks are be obtained, which are represented by discrete time intervals. To complete the relocation tasks, it is necessary to better organize the staff and design a suitable time window. We use p to represent the vehicle relocation tasks $(i_k,t,j_k,s) \in A$. The pick-up station of task p is station i_k, and the drop-off station of task p is station j_k. The departure time interval is denoted by p^t, and the arrival time interval is denoted as p^s. The service time of this relocation task p is denoted as $p^{tr} = \delta \cdot (s-t)$. For the vehicle relocation task p, the departure time p^λ can be obtained using Eq. (24) and (25).

$$\left\lceil \frac{p^\lambda}{\delta} \right\rceil = p^t \tag{24}$$

$$\delta \cdot (p^t - 1) \le p^\lambda \le \delta \cdot p^t \tag{25}$$

The departure time window for task p can then be expressed by Eq. (26) and (27), where p^e denotes the earliest departure time and p^f denotes the latest departure time of task p.

$$p^e = \delta \cdot (p^t - 1) \tag{26}$$

$$p^f = \delta \cdot p^t \tag{27}$$

Table 3
Notations in the staff rebalancing model.

Parameters	
$V^{'}$	set of dummy stations (relocation tasks)$V^{'} = \{1, 2, \cdots, v^{'}\}$
Ω	set of depots for multiple companies $\Omega = \{1, 2, \cdots, \omega\}$ (typically there is one depot where the office of the company is located but there could be more)
p, q	indexes of dummy stations (relocation tasks), $p, q \in V^{'}$
L_p	number of relocation staff at depot $p, p \in \Omega$
$s^{'}_{pq}$	staff movement distance between task p and task q
$v^{'}$	the driving speed of an electric scooter used by the staff
η_{dc}	the cost of driving an electric scooter per kilometer
η_{pc}	the penalty cost for not performing one relocation task
p^e	the earliest departure time of task p
p^f	the latest departure time of task p
p^{tr}	the service time of the relocation task p
$\mathscr{M}$	a big number
Decision variables	
y_{pq}	binary variable, 1 if a staff member moves from the drop-off station of task p to the pickup station of task q. This denotes that the relocation staff performs both relocation tasks p and q
p^{λ}	the departure time of task p
u_p	binary variable, taking value 1, if task p is performed

3.2.2. Phase 2: Staff rebalancing optimization

Based on the relocation tasks arranged in Phase 1, the staff should move between stations to perform the vehicle relocation tasks. Fig. 5 shows the staff rebalancing process. For each relocation task, the pick-up station is represented by a circle and the drop-off station is represented by a square. The vehicle relocation process from the pick-up station to the drop-off station is depicted by the red arcs. The staff should be relocated between the two vehicle relocation tasks, as depicted by the blue arcs. After the staff completed relocation Task 1, he/she moves to the pick-up station of Task 2 using the folding bicycle or the electric scooter. Therefore, the staff rebalancing route is from the drop-off station of Task 1 to the pick-up station of Task 2.

The staff rebalancing optimization problem is modeled in Phase 2, where the staff are reasonably scheduled to the appropriate stations to complete the vehicle relocation tasks. We assume that the staff moves between different tasks using the electric scooter. It should be noted that there may be multiple relocation tasks at a single carsharing station. If this happens, we create a set of dummy stations, $V^{'}$, which ensures that there is only one vehicle relocation task at each dummy station. The notations used in the staff rebalancing model are listed in Table 3.

The objective function of the Phase 2 model is:

$$Minimize(\Pi_2) = \eta_{dc} \cdot \sum_{p \in \Omega \cup V^{'}} \sum_{q \in \Omega \cup V^{'}} y_{pq} \cdot s^{'}_{pq} + \eta_{pc} \cdot \sum_{p \in V^{'}} (1 - u_p) \tag{28}$$

Subject to:

$$\sum_{q \in V^{'}} y_{pq} \leq L_p, \ \forall p \in \Omega \tag{29}$$

$$\sum_{p \in \Omega} \sum_{q \in V^{'}} y_{pq} = \sum_{p \in \Omega} \sum_{q \in V^{'}} y_{qp} \tag{30}$$

$$\sum_{q \in V^{'}} y_{pq} - \sum_{q \in V^{'}} y_{qp} = 0, \ \forall p \in V^{'} \tag{31}$$

$$\sum_{q \in V^{'}} y_{pq} - u_p = 0, \ \forall p \in V^{'} \tag{32}$$

$$p^{\lambda} + p^{tr} + \left(\frac{s^{'}_{pq}}{v^{'}}\right) \leq \mathscr{M}(1 - y_{pq}) + q^{\lambda}, \forall p, q \in V^{'}, p \neq q \tag{33}$$

$$p^e \leq p^{\lambda} \leq p^f, \forall p \in V^{'} \tag{34}$$

$$y_{pq} \in \{0, 1\}, \forall p, q \in V^{'} \tag{35}$$

$$u_p \in \{0, 1\}, \forall p \in V^{'} \tag{36}$$

The objective function (28) minimizes the rebalancing costs of the staff between tasks using the electric scooter and the penalty cost for not fulfilling the relocation tasks. Constraints (29) set the upper bound of the staff in each depot, which are available to perform the relocation tasks. Constraints (30) imply that each relocation staff starts at their initial depot and returns to the final depot at the end of

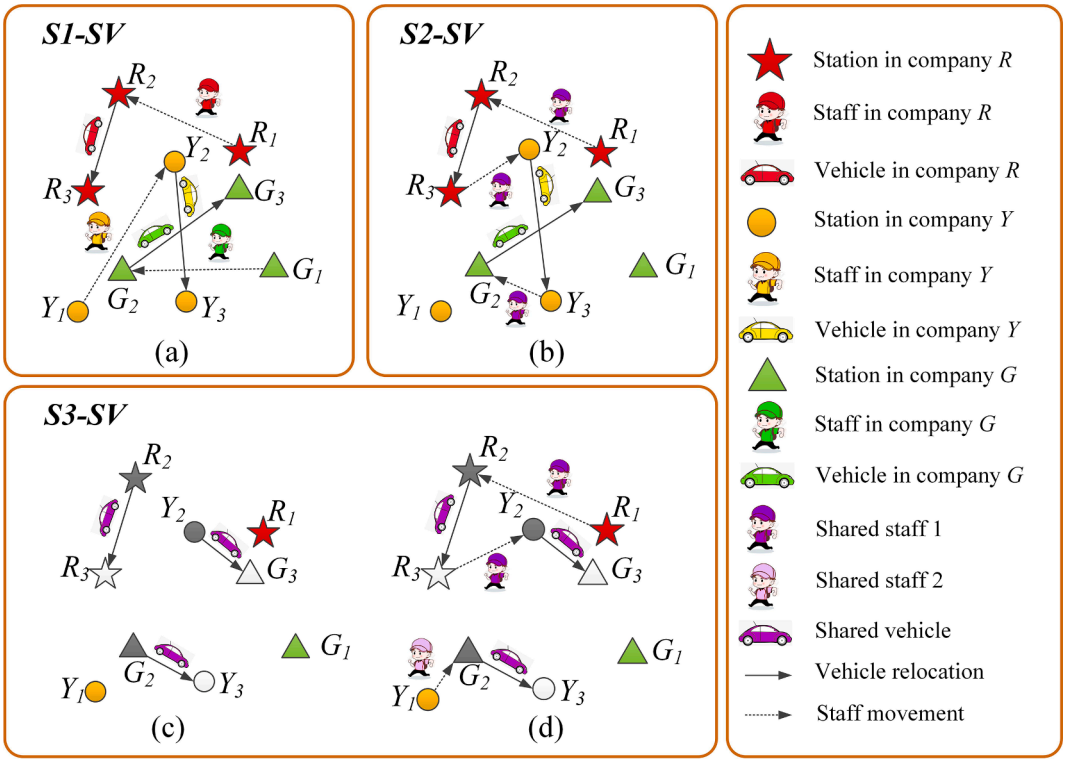

Fig. 6. Illustration of the multi-company cooperative relocation.

the stage. Constraints (31) and (32) ensure that the relocation task has to be performed at most once during each stage. Constraints (33) establish the relationship of the staff departure time to serve tasks, and constraints (34) ensure that the solutions obey the time window constraints of each task. Constraints (35) and (36) set the domains of variables y_{pq} and u_p.

3.3. Multi-company cooperative relocation

Multi-company cooperative relocation considers that multiple carsharing companies can share vehicles, stations, and staff to increase shared vehicle usage and staff working efficiency with cooperative schemes. In Fig. 6, we present an example of a multi-company relocation strategy with three carsharing companies, named $R, G,$ and Y. Three types of cooperative relocation strategies are considered.

The first strategy is the shared vehicle relocation without cooperation (S1-SV), where neither the vehicles nor the staff are shared. Each company relocates the shared vehicles and rebalances the staff independently without cooperation. For example, in Fig. 6 (a), we suppose there are three stations in each company, e.g., R_1, R_2, R_3. Company R has a vehicle relocation task from station R_2 to station R_3. Similar relocation tasks should also be carried out from station Y_2 to station Y_3 at the company Y and from station G_2 to station G_3 at the company G. However, the staff of the three companies are located at the stations R_1, Y_1 and G_1 respectively. Therefore, the staff at the station R_1 must travel from R_1 to R_2 using an electric scooter to complete the vehicle relocation task from R_2 to R_3. Staff from other companies perform similar tasks to ensure that shared cars are deployed between the corresponding stations.

The second shared vehicle relocation strategy (S2-SV) considers staff cooperation. The relocation staff are shared, which means that they can perform the relocation tasks of different companies. With this strategy, the work efficiency of the staff is potentially increased, reducing the number of staff idling in the stations and waiting for the next relocation task. Although the staff can relocate vehicles from different companies, the shared vehicles from different companies should still be parked at the stations of the corresponding company. For example, in Fig. 6 (b), assuming that the relocation tasks are all completed within the time window, the shared staff (in purple) will first use the electric scooter to travel from station R_1 to station R_2, and then complete the vehicle relocation task from station R_2 to station R_3. After completing the relocation task from company R, he/she uses an electric scooter to reach the adjacent station Y_2 and complete the relocation task from station Y_2 to station Y_3. Similarly, after completing the relocation task from company Y, he/she comes to the adjacent station G_2 and completes the relocation task from station G_2 to station G_3. It can be seen that the strategy of staff sharing can effectively improve the staff work efficiency in the current carsharing system and reduce the total number of employed staff.

In the third shared vehicle relocation strategy (S3-SV), the staff and vehicles are shared. The vehicles can be parked at the stations of different carsharing companies, and the staff can perform the relocation tasks of different carsharing companies, as shown in Fig. 6 (c)

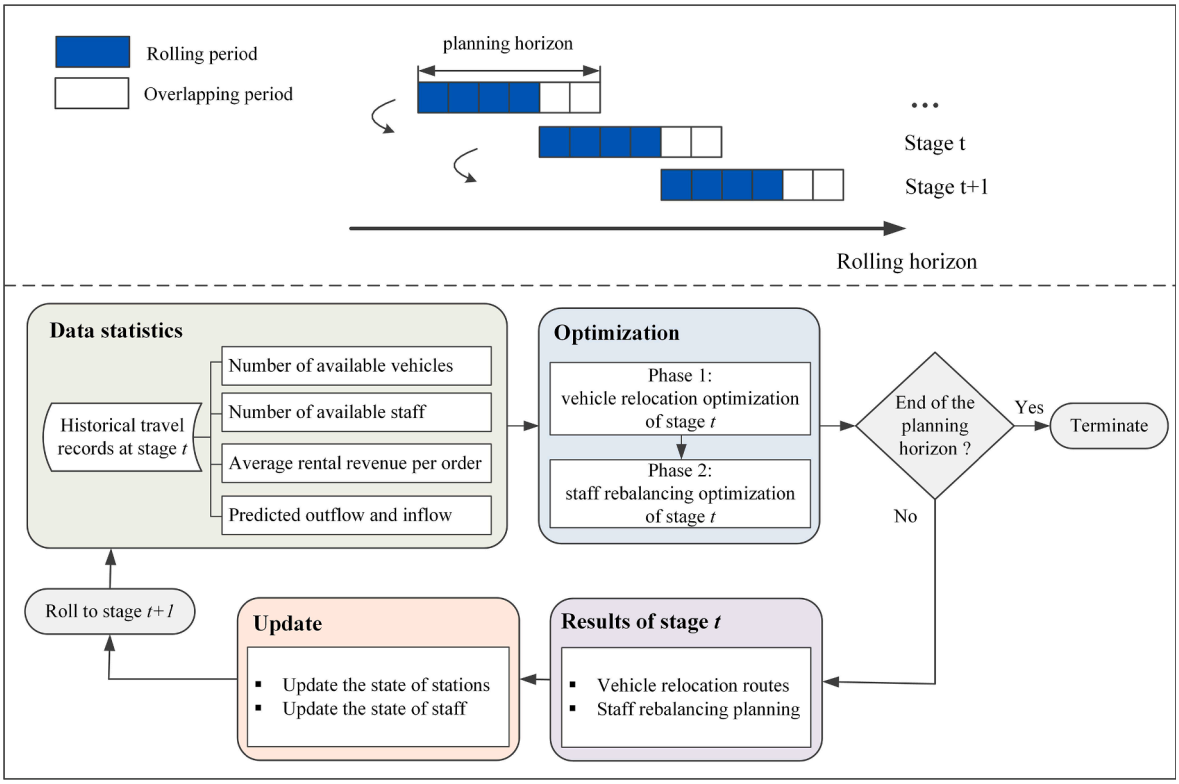

Fig. 7. Successive stages planning with the rolling horizon approach.

and (d). Similar to the scenario settings in Fig. 6 (a) and (b), there are redundant vehicles at stations R_2, Y_2, and G_2 (grey), and stations R_3, Y_3, and G_3 (white) need vehicles. Thus, the staff should perform the vehicle relocation tasks from stations R_2, Y_2, and G_2 to stations R_3, Y_3, and G_3. Strategy 3 allows the vehicle relocation around nearby stations, even though they belong to different companies. Therefore, Fig. 6 (c) shows the optimal vehicle relocation routes based on our proposed Phase 1 model, where the optimized vehicle relocation routes are from station R_2 to station R_3, from station G_2 to station Y_3, and from station Y_2 to station G_3. The Phase 2 model arranges the staff rebalancing routes. Initially, the staff of the three companies are located at stations R_1, Y_1, and G_1 respectively. In Fig. 6(d), the shared staff 1 travels from station R_1 to station R_2 using his/her electric scooter, completing the vehicle relocation task from station R_2 to station R_3. Thereafter, he/she uses the electric scooter to reach the adjacent station Y_2, completing the relocation task from station Y_2 to station G_3. Another shared staff 2 starts from station Y_1 to station G_2 to complete the vehicle relocation task from station G_2 to station Y_3.

4. Solution method

4.1. Rolling horizon algorithm

We adopt a rolling horizon approach to handle the time-varying demand of shared car trips during the day, which decomposes the relocation route for the entire service time horizon into smaller connected stages (Shui and Szeto, 2017). At each rolling horizon, the assignment of tasks is decided using the fore view regarding the forecasted demand (with the AE-TGCN model) and the updated available vehicles and staff members. Fig. 7 shows the successive planning stages within the rolling horizon approach. Each stage covers a rolling period with a fixed duration and an overlapping period (except for the last stage with no overlapping period).

At the beginning of each stage, a set of historical travel records is first used to derive all statistics, such as the predicted outflow and inflow travel demand, the number of available vehicles and staff distributed among stations, etc., which are the inputs for the optimization model. Thereafter, the Phase 1 model determines the vehicle relocation tasks, and the Phase 2 model schedules the staff to perform these tasks. After solving the two-phase optimization model, the optimal vehicle relocation and staff rebalancing routes are planned, which will be used to update the initial inventory of vehicles and staff at each station for the next stage. The rolling horizon planning allows the new data from the current stage to join the historical dataset, and the nearest set of data will be used to derive new statistics, which will be the new inputs for the proposed model to search for the new optimal relocation strategy for the next stage (Huo et al., 2020). The outline of the solution procedure is provided as follows:

Step 1: Obtain the predicted inflow/outflow demand and the available vehicles and staff at each station for each period of stage t.

Step 2: Determine the vehicle relocation tasks and routes in the current stage t using the Phase 1 model with the branch-and-cut algorithm.
Step 3: Arrange the staff to perform the relocation tasks in Step 2 and plan the staff rebalancing activities in the current stage t using the Phase 2 model with the ALNS based heuristics.
Step 4: Store the vehicle relocation routes and staff activities, and update the stations' demand, available vehicles, and the number of staff at each station.
Step 5: If the current stage is not the last stage, then $t = t+1$ and go to Step 2. Otherwise, the algorithm stops and outputs the results.

4.2. The ALNS based heuristic

In the Phase 2 model, several relocation tasks may appear at the same carsharing station. Thus, many dummy stations are set up to ensure that each dummy station has only one vehicle relocation task. In addition, the staff start from different depots to perform the relocation tasks in real-world carsharing companies. Commercial solvers such as CPLEX may fail to solve large-scale instances within an acceptable time. Adaptive large neighborhood search (ALNS) is a *meta*-heuristic algorithm that has been successfully adopted to solve the complex routing and scheduling problems (Luo et al., 2016; Sun et al., 2020). In this study, the ALNS based heuristic approach is implemented to solve the staff rebalancing model.

The ALNS heuristic applies multiple destroy and repair operators during the neighborhood search process, which are chosen according to the adaptive mechanism. In each iteration, the destroy operators remove a part of the incumbent solution, and the repair operators construct a new solution. The removed part can be viewed as a parameter that controls the neighborhood size. Constructing a larger neighborhood increases the opportunity to find better solutions but requires more training time. In this study, three destroy operators are developed to ruin the current solution. The random destroy operator randomly removes relocation tasks from the current solution, which provides diversification to enlarge the search space. The idea of the worst-cost destroy operator is to remove the worst parts of the current solution, that is, those tasks that cause the high staff rebalancing costs, hoping that the great cost can be eliminated in the following repair process. To arrange for the staff to perform the vehicle relocation tasks within suitable time windows, the worst-time destroy operator removes the tasks with long waits or delayed service start times (Demir et al., 2012; Sun et al., 2020). Accordingly, three repair operators are constructed to repair the destroyed solutions. To diversify the search, the random repair operator inserts the unserved tasks into randomly selected positions of the route at each step. The greedy repair operator inserts the unserved tasks in the best possible position of the routes that can minimize the rebalance costs. The regret repair operator inserts the unserved tasks considering the regret value, which is the difference between the objective function values incurred by inserting the unserved task to its best position and its second-best position (Sun et al., 2020).

The adaptive mechanism improves the probability of selecting a better-performing operator, which is based on a roulette wheel selection. When a higher-quality solution is obtained with an operator, a higher score is given to the promising operator to enhance the probability of being selected again while the selection probabilities of unpromising operators are reduced. Let Ψ and Φ denote the sets of the destroy operators and repair operators, respectively, and let $\psi \in \Psi$ be the destroy operator and $\varphi \in \Phi$ be the repair operator. ω_{ψ}^{κ} and $\omega_{\varphi}^{\kappa}$ are the weights of the destroy and repair operators in the κ iteration, respectively, which are set equal to 1 at the beginning. We define π_{ψ}^{κ} as the total score collected by the destroy operator ψ in the κ iteration, and π_{φ}^{κ} as the total score collected by the repair operator φ in the κ iteration. The total scores π_{ψ}^{κ} and π_{φ}^{κ} are adjusted based on the newly obtained solution, where the reward parameters $\varrho_1, \varrho_2,$ and $\varrho_3 (\varrho_1 \geq \varrho_2 \geq \varrho_3)$ are introduced (Luo et al., 2016; Sun et al., 2020).

ϱ_1 : The new solution is the best one found so far.
ϱ_2 : The new solution is better than the current solution.
ϱ_3 : The new solution is worse than the current solution but is accepted.

At the end of the κ iteration, ω_{ψ}^{κ} is updated using Eq. (37). u_{ψ}^{κ} denotes the number of times the destroy operator ψ has been invoked during the iterations, and $\rho \in [0,1]$ controls the influence of the operator's historical performance. In addition, the repair operator $\omega_{\varphi}^{\kappa}$ follows a similar updating process with Eq. (38).

$$\omega_{\psi}^{\kappa+1} = \begin{cases} (1-\rho)\cdot\omega_{\psi}^{\kappa} + \rho\cdot\dfrac{\pi_{\psi}^{\kappa}}{u_{\psi}^{\kappa}} & if \quad u_{\psi}^{\kappa} > 0 \\ (1-\rho)\cdot\omega_{\psi}^{\kappa} & if \quad u_{\psi}^{\kappa} = 0 \end{cases} \tag{37}$$

$$\omega_{\varphi}^{\kappa+1} = \begin{cases} (1-\rho)\cdot\omega_{\varphi}^{\kappa} + \rho\cdot\dfrac{\pi_{\varphi}^{\kappa}}{u_{\varphi}^{\kappa}} & if \quad u_{\varphi}^{\kappa} > 0 \\ (1-\rho)\cdot\omega_{\varphi}^{\kappa} & if \quad u_{\varphi}^{\kappa} = 0 \end{cases} \tag{38}$$

The simulated annealing (SA) algorithm is always combined in the ALNS heuristic framework. To jump out of the current local optimum, the SA can accept the worse solutions with probability $\mathscr{P}$, in Eq. (39). The acceptance probability $\mathscr{P}$ comprises two parameters $\mathscr{t}$ and $\Delta cost$. $\mathscr{t}$ is called the temperature, and it gradually decreases during the search. $\Delta cost$ is the difference in the objective function between the new solution and the current solution. In this study, an enhanced simulated annealing (ESA) algorithm is

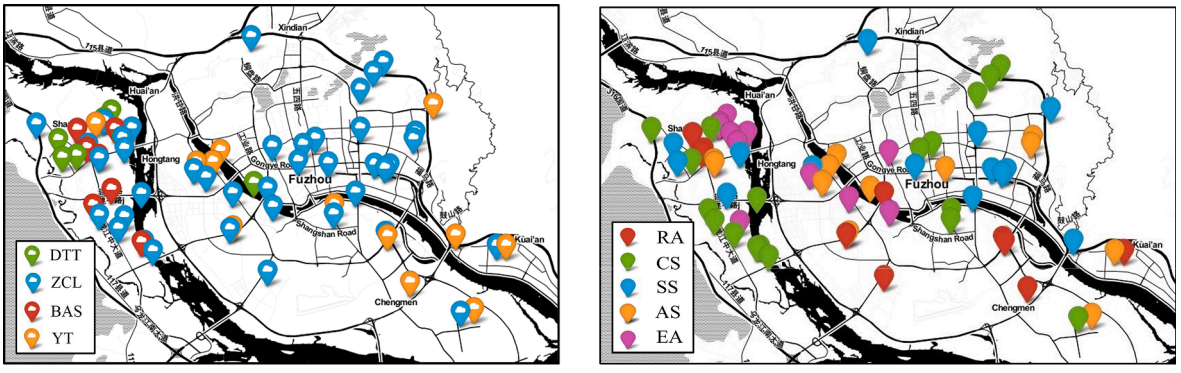

Fig. 8. The distribution of carsharing stations in Fuzhou city: (a) station locations; (b) land-use characteristics.

embedded ALNS heuristic framework, where the ESA uses a modified acceptance probability $\mathscr{P}(r_{current}, r_{new}, r_{best}, \mathscr{t})$ in Eq. (40) to obtain higher-quality solutions considering not only the gap to the current solution, $\Delta cost$, but also the gap to the optimal solution that has been reached, $\Delta cost^{'}$.

$$\mathscr{P} = exp(-\Delta cost/\mathscr{t}) \tag{39}$$

$$\mathscr{P}(r_{current}, r_{new}, r_{best}, \mathscr{t}) = \frac{exp(-\Delta cost/\mathscr{t})}{exp(-\Delta cost^{'}/\mathscr{t})} \tag{40}$$

where $\Delta cost = \Pi_2(r_{current}) - \Pi_2(r_{new})$; $\Delta cost^{'} = \Pi_2(r_{best}) - \Pi_2(r_{new})$; $r_{current}$ is the current solution; r_{new} is the new neighborhood solution; r_{best} is the current best solution, and $\Pi_2(\cdot)$ is the objective function of the Phase 2 model.

Algorithm 1. The framework of ALNS based heuristic, ALNS-ESA

input: destroy operators Ψ, repair operators Φ, initial temperature $\mathscr{t}_{init}$, cooling rate τ
Generate an initial solution by using the Clarke and Wright algorithm r_{init}
Initialize probability for the destroy operators Ψ and repair operators Φ
Let $r_{current} = r_{init}, r_{best} = r_{init}$; the temperature $\mathscr{t} = \mathscr{t}_{init}$
while the time limit has not been reached **do**
  Select a destroy operator ψ with probability ω_{ψ}^{κ}
  Let $r_{new}^{'}$ be the solution obtained by applying the destroy operator ψ to $r_{current}$
  Select a repair operator φ with probability $\omega_{\varphi}^{\kappa}$
  Let r_{new} be the solution obtained by applying the repair operator φ to $r_{new}^{'}$
  if $\Pi_2(r_{new}) < \Pi_2(r_{current})$ **then**
    $r_{current} = r_{new}$
    $\Delta cost = \Pi_2(r_{current}) - \Pi_2(r_{new})$
    if $\Pi_2(r_{new}) < \Pi_2(r_{best})$ **then**
      $r_{best} = r_{new}; cost_{best} = \Pi_2(r_{new})$
      $\Delta cost^{'} = \Pi_2(r_{best}) - \Pi_2(r_{new})$
  else
    $r_{current} = r_{new}$ with probability $\varepsilon = \frac{exp(-\Delta cost/T)}{exp(-\Delta cost^{'}/T)}$
  Update the temperature $\mathscr{t} = \tau \cdot \mathscr{t}$
  Update probabilities using the adaptive probability adjustment procedure
end while
return $r_{best}, cost_{best}$

The detailed process of the ALNS based heuristic, ALNS-ESA, is presented in Algorithm 1. The ALNS-ESA algorithm is numerically compared with the exact algorithm (using CPLEX 12.10) and other heuristics, such as SA (Wei et al., 2018), tabu search (Ho and Szeto, 2014), and ant colony optimization (Oliveira et al., 2021) with small-scale examples in Appendix A. Results show that the ALNS-ESA algorithm can obtain better solutions compared with the SA, tabu search and ant colony optimization algorithm in a reasonable time.

5. Data description

We collect 6-month carsharing travel records from January 1, 2018, to May 31, 2018, in Fuzhou, which is the capital city of the Fujian Province in China. The travel records are from four carsharing companies, including the companies DTT, ZCL, BAS, and YT. The

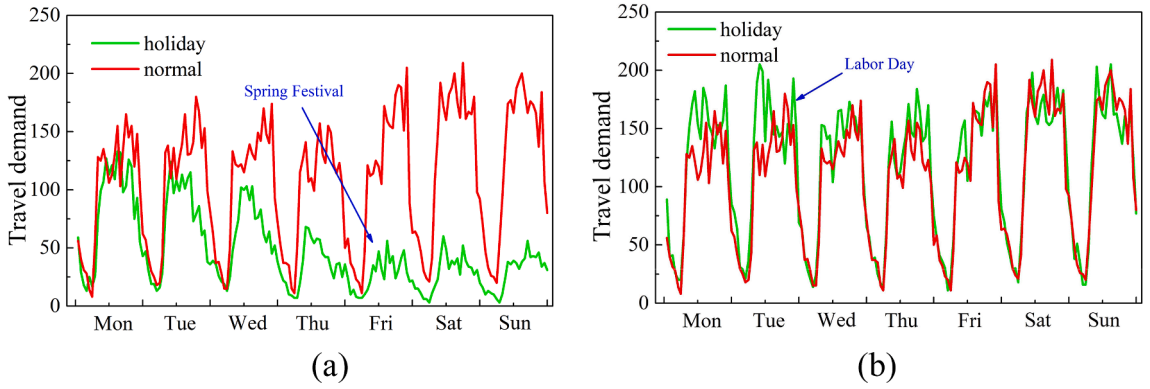

Fig. 9. Temporal usage patterns of shared cars: (a) on normal days; (b) on holidays.

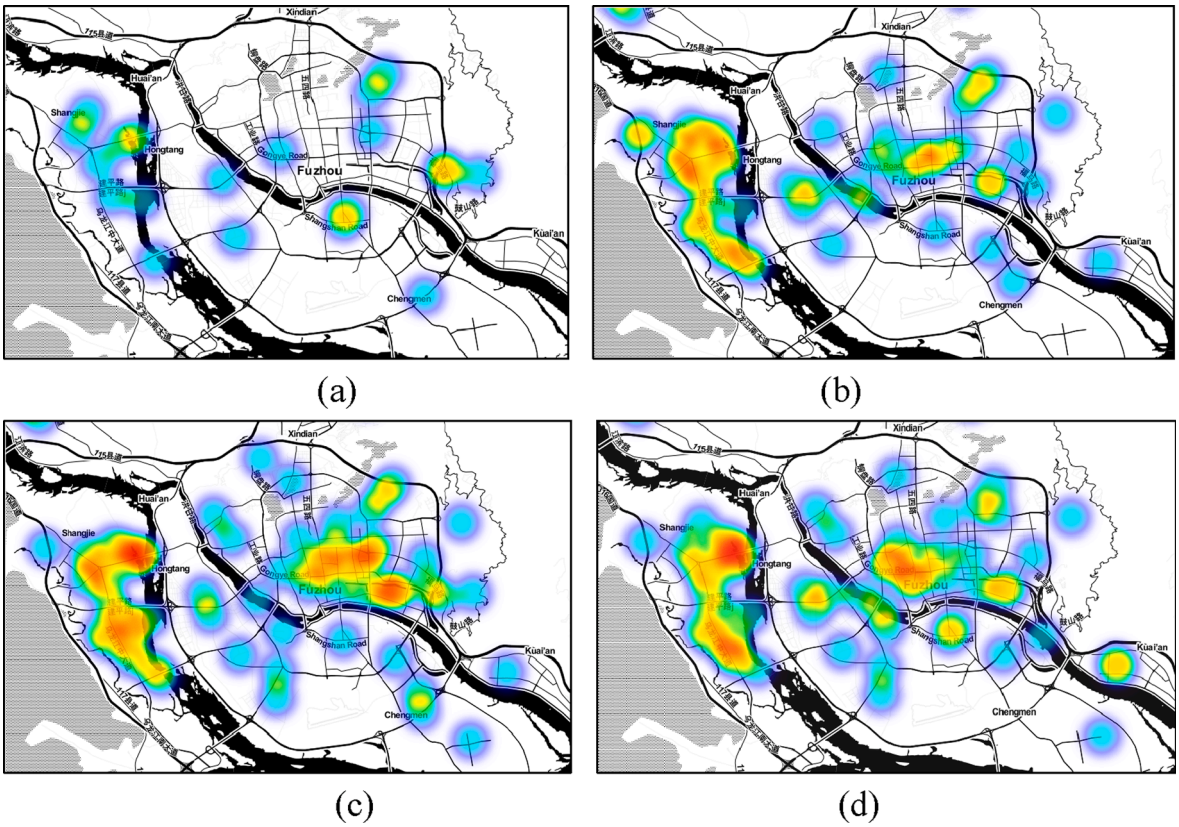

Fig. 10. The spatial and temporal distribution of carsharing travel demand during a normal day in Fuzhou: (a) 6:00–7:00; (b) 8:00–9:00; (c) 12:00–13:00 and (d) 20:00–21:00.

attributes of the data include the company name, the order number, vehicle ID, the user's ID, pick-up time, return time, pick-up station, return station, travel time, travel distance, and travel costs. The distribution of the 67 stations from the four carsharing companies is shown in Fig. 8 (a).

The point-of-interest (POI) data and the weather data for the corresponding days are collected from the web crawling framework developed using Python. The POI dataset provides information on land-use characteristics surrounding the selected stations. The categories can be divided into five types: catering services (CS), enterprise areas (EA), shopping services (SS), auto service (AS), and residential areas (RA). We crawl the POI within 500 m of each station and tag the most frequent POI type around the stations as a land-use characteristic (Fig. 8(b)). The weather conditions are divided into five categories: sunny, cloudy, light rain, moderate rain, and heavy rain.

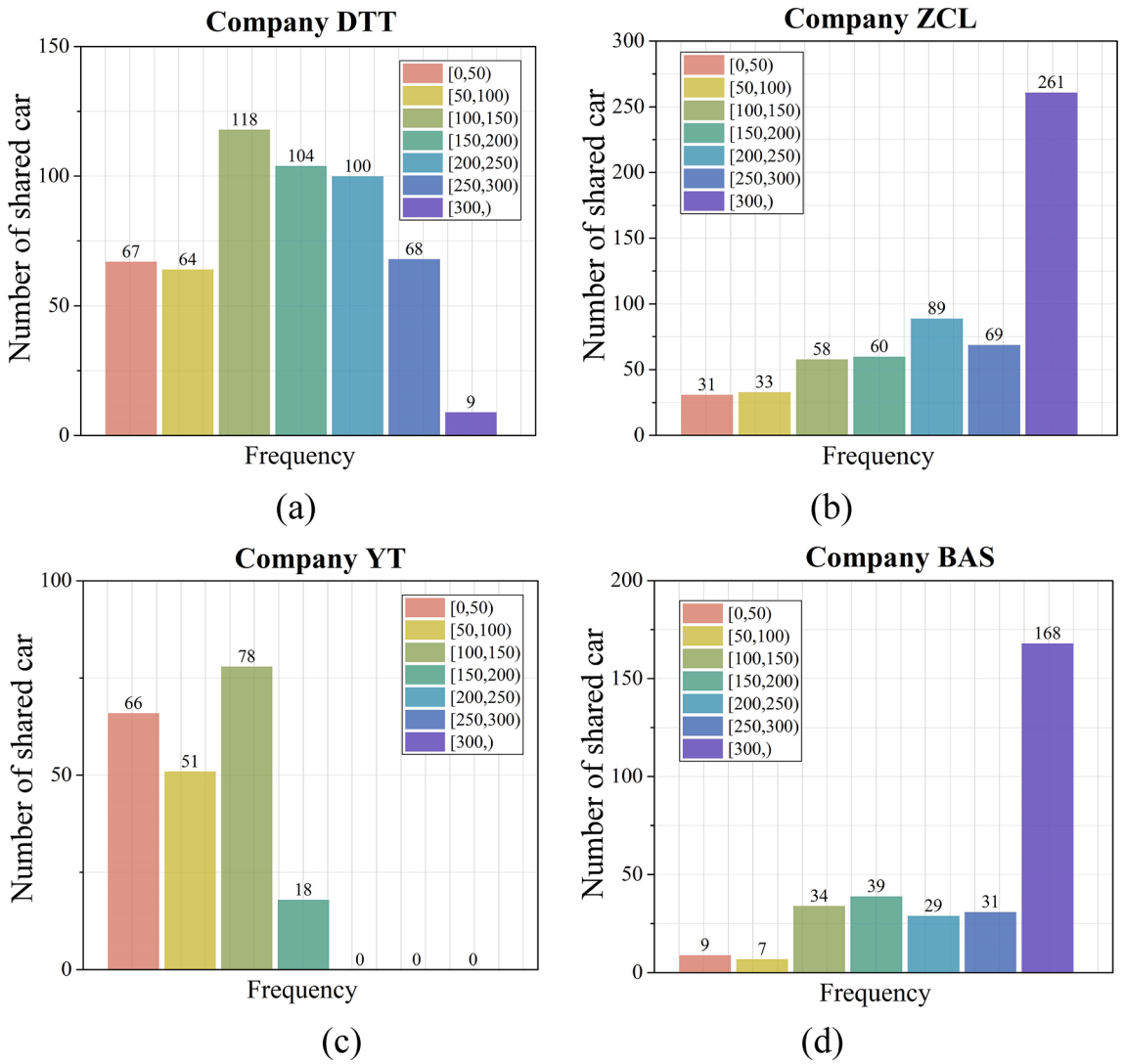

Fig. 11. The usage frequency of shared car use in four companies: (a) Company DTT; (b) Company ZCL; (c) Company YT; (d) Company BAS.

5.1. Spatial and temporal carsharing trip patterns

Fig. 9 analyzes the temporal characteristics of shared car trips. In general, during normal days, the number of shared car trips on weekends is slightly larger than that on weekdays. There are no morning and evening peak hours on weekdays because shared cars are not the main travel mode for commuting compared with public transportation, such as the subway and bus. The holiday travel patterns of shared cars can be reflected in the travel data. Fig. 9 (a) shows the weekly travel demand during the Spring Festival (February 16, 2018). During these days, people usually gather with their families, so the travel demand for shared cars will be significantly reduced. Fig. 9 (b) shows the carsharing travel demand during Labor Day (May 1, 2018). There is a 3-day holiday on International Labor Day, and people use these holidays for travel, and the number of trips greatly increases. The spatial distribution of carsharing travel demand during a normal day is shown in Fig. 10. It can be seen during the period 6:00–7:00, there are fewer carsharing trips. The carsharing demand gradually increases during 8:00–9:00, and the travel hotspots become obvious during the daytime. During 20:00–21:00, a considerable number of carsharing trips also exist.

5.2. Vehicle usage patterns in different companies

The user should first register as a member of the carsharing company before using the shared car. For example, at Company DTT, a deposit of $185 is required for registration, which makes most users only register as a member of one carsharing company. From the analysis of 6-month shared car travel data, there are 38,860 registered users (each with a unique user ID), of which only 2,365 people have registered for two companies, accounting for a total of 6.08%. Only 95 users have registered in three or more companies at the

Table 4
Multi-step prediction performance comparison on different time steps.

Model	30 min (one step)		60 min (two steps)		120 min (four steps)	
	RMSE	MAE	RMSE	MAE	RMSE	MAE
(a) inflow prediction						
HA	0.9835	0.5923	0.9835	0.5923	0.9835	0.5923
ARIMA	1.0762	0.9750	1.1090	0.9758	1.2088	0.9852
SVR	0.9374	0.5388	0.9415	0.5798	0.9572	0.5882
GRU	0.9235	0.5192	0.9318	0.5631	0.9328	0.5774
GCN	0.9415	0.5867	0.9636	0.6143	0.9828	0.6110
TGCN	0.8641	0.5071	0.8736	0.5301	0.8714	0.5320
AE-TGCN	**0.8414**	**0.4743**	**0.8483**	**0.5102**	**0.8580**	**0.5252**
(b) outflow prediction						
HA	0.9615	0.5846	0.9615	0.5846	0.9615	0.5846
ARIMA	1.0649	0.9573	1.0792	0.9589	1.1207	0.9765
SVR	0.9314	0.5035	0.9391	0.5635	0.9418	0.5629
GRU	0.9286	0.5155	0.9290	0.5641	0.9388	0.5608
GCN	0.9581	0.5393	0.9686	0.5904	0.9714	0.6005
TGCN	0.8571	0.5035	0.8708	0.5215	0.8636	0.5294
AE-TGCN	**0.8352**	**0.4878**	**0.8439**	**0.5045**	**0.8407**	**0.5019**

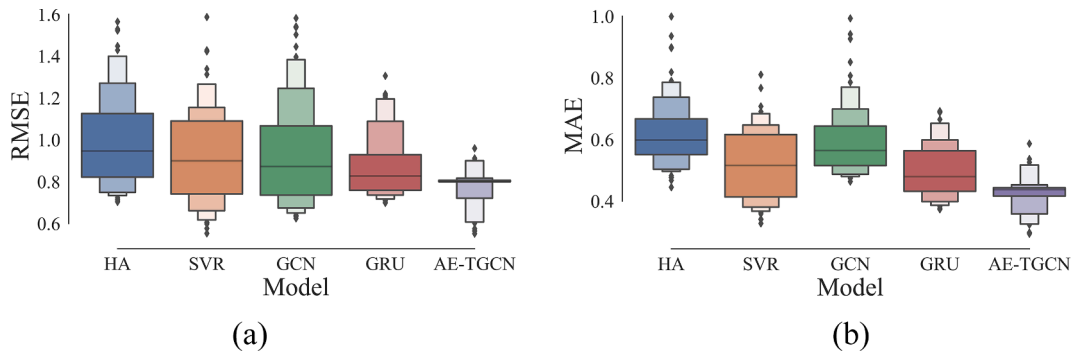

Fig. 12. Prediction performance of 67stations on 30 min horizon: (a) RMSE of inflow prediction; (b) MAE of inflow prediction.

same time, accounting for 0.24%. Fig. 11 shows the usage frequency of shared cars in the four companies. The average usage frequencies of Company DTT, ZCL, YT, BAS are 155.82, 279.03, 82.93, and 300.25, respectively. Specifically, the shared cars in two companies, Company ZCL and Company BAS, have a high usage frequency, and 261 and 168 vehicles are used more than 300 times during the statistical period in Fig. 11(b) and (d). However, the vehicles in Company YT are rarely used, and each vehicle is used less than 200 times, as shown in Fig. 11(c). Owing to the lack of effective cooperation among these companies and effective relocation strategies, more shared vehicles are idling at some stations, resulting in low usage frequency.

6. Case study

6.1. Multi-step prediction performance of AE-TGCN

In this section, we estimate the multi-step travel demand prediction model of AE-TGCN using the real-world carsharing usage data. The carsharing network structure is represented by an adjacency matrix with 67 stations, which describes the spatial relationships among the stations. The shared car usage data is resampled every 30 min to describe the inflow and outflow travel demand at each station. The land-use characteristics and weather conditions are integrated to improve the model's ability to perceive external factors. The proposed AE-TGCN model is compared with several benchmark methods, including the historical average (HA), autoregressive integrated moving average (ARIMA), support vector regression (SVR), GCN, and GRU. Deep learning models are developed using Python TensorFlow. The demand forecast model is evaluated by two evaluation indicators, the root mean square error (RMSE) and the mean absolute error (MAE), as shown in Eq. (41) and (42).

$$RMSE = \sqrt{\frac{1}{MN}\sum_{j=1}^{M}\sum_{i=1}^{N}\left(y_{i,j} - \widehat{y_{i,j}}\right)^2} \tag{41}$$

Table 5
Result comparison of different relocation strategies on working days (April 3, 2018).

Relocation strategies	S1-SV	S2-SV	S3-SV
Profit (dollars per day)	7062.10	7499.20	8862.32
Total cost (dollars per day)	4012.84	3575.74	2212.62
(a) Result of Phase 1			
Revenue (dollars per day)	11074.94	11074.94	11074.94
Pickup demand (per day)	1178	1178	1178
Return demand (per day)	1100	1100	1100
Number of relocation tasks	336	336	240
Vehicle relocation cost (dollars per day)	1730.34	1730.34	715.26
Total relocation distance (km)	576.78	576.78	238.42
Average relocation distance (km)	1.72	1.72	0.99
(b) Result of Phase 2			
Staff movement cost (dollars per day)	2282.50	1845.40	1497.36
Maximum number of required staff	15	9	8
Total staff movement distance (km)	1141.25	922.70	748.68
Total staff waiting time (min)	1802.43	1036.39	763.66

$$MAE = \frac{1}{MN}\sum_{j=1}^{M}\sum_{i=1}^{N}\left|y_{i,j} - \widehat{y_{i,j}}\right| \tag{42}$$

where $y_{i,j}$ and $\widehat{y_{i,j}}$ represent the real travel demand and predicted travel demand of the j-th time samples in the i-th station. M is the number of time samples; N is the number of stations.

Table 4 shows the multi-step prediction performance of the proposed model and benchmark algorithms for 30 min, 60 min, and 120 min ahead forecasting the inflow and outflow travel demands. For different prediction intervals, the performance of HA is invariant because it only depends on the historical data. The GRU model introduces the gating mechanism to control the temporal memory, which has better prediction precision than other baselines, such as the HA, ARIMA, SVR models. In addition, the GRU model outperforms the GCN model, verifying that the temporal features are important in short-term demand prediction tasks. The TGCN model captures the spatial and temporal features simultaneously with the GCN and GRU modules. For the 30 min inflow demand forecasting task, the RMSE errors of the TGCN model are reduced by approximately 8.22% and 6.43% compared with the GCN model and GRU models, respectively. Enhanced by the attention mechanism, the AE-TGCN model has the best prediction performance, and the prediction errors of both RMSE and MAE are smaller than those of the TGCN model. Under different prediction horizons, the ARIMA model performs the worst because of the error accumulation, while the error increase of the AE-TGCN model is small, which shows a certain degree of stability for multi-step prediction tasks. Fig. 12 illustrates the inflow prediction error of the 67 stations on a 30 min horizon. The prediction error is large in some stations with the HA, SVR, and GCN models, while it decreases by capturing the spatiotemporal characteristics with the AE-TGCN model.

6.2. Relocation results with different cooperative strategies

At each rolling horizon, based on the predicted inflow and outflow demand, we determine the vehicle relocation tasks and schedule the staff to perform these tasks using the proposed two-phase vehicle relocation and staff rebalancing model in Section 3.2. We test our model and cooperative relocation strategies using the multi-company carsharing travel records in Fuzhou. Considering the large travel demand at night (e.g., in Fig. 10 (d)), the dynamic vehicle relocation and staff rebalancing operation during the day is set for the period 8:00–24:00. There are 67 stations from four carsharing companies, and each station has 10 parking spaces. We assume that each company employs 10 relocation staff to perform the relocation tasks during the day. The vehicle relocation cost α in the Phase 1 model is set to \$3/km. The penalty for not fulfilling one request β is \$20. The driving speed of the staff relocating a vehicle ν is set to 30 km/h. In the Phase 2 model, the staff uses an electric scooter to move between various relocation tasks. The staff moving speed in those trips ν' is set to 20 km/h, and the staff moving cost η_{dc} is \$2/km. The penalty cost for not performing one relocation task η_{pc} is \$20. Based on the above parameter settings, we solve the two-phase vehicle relocation and staff rebalancing model and obtain the following results.

6.2.1. Result comparison of cooperative relocation strategies

As described in Section 3.3, the vehicles, stations, and staff are allowed to be shared according to the cooperative relocation strategies that have been explained previously. Table 5 shows the results of the different relocation strategies on a working day (Tuesday, April 3, 2018). In general, during the day, the total fulfilled pick-up demand at 67 stations is 1,100, while the return demand is 1,178, resulting in a total revenue of \$11,074.94. The vehicles are only allowed to be relocated between stations in the same company with S1-SV (the relocation strategy without cooperation) and S2-SV (the relocation strategy with only shared staff). Hence, in the results of the Phase 1 model with S1-SV and S2-SV, a total of 336 vehicle relocation tasks should be performed by the four companies to prevent situations in which there are no shared vehicles to use or no space for vehicle parking, with an average relocation distance of 1.72 km per task. However, the vehicles are allowed to be relocated between stations of different companies with cooperative strategy S3-SV (the relocation strategy with shared staff and vehicles). That is, relocation tasks can be performed in nearby

Table 6
Result comparison of different relocation strategies on holidays (May 1st, 2018).

Relocation strategies	S1-SV	S2-SV	S3-SV
Profit (dollars per day)	9127.17	9682.27	10933.77
Total cost (dollars per day)	4043.06	3487.96	2236.46
(a) Result of Phase 1			
Revenue (dollars per day)	13170.23	13170.23	13170.23
Pickup demand (per day)	1294	1294	1294
Return demand (per day)	1284	1284	1284
Number of relocation tasks	431	431	342
Vehicle relocation cost (dollars per day)	1731.32	1731.32	587.40
Total relocation distance (km)	577.11	577.11	195.80
Average relocation distance (km)	1.34	1.34	0.57
(b) Result of Phase 2			
Staff movement cost (dollars per day)	2311.74	1756.64	1649.06
Maximum number of required staff	18	13	10
Total staff movement distance (km)	1155.87	878.32	824.53
Total staff waiting time (min)	2061.15	1467.64	869.23

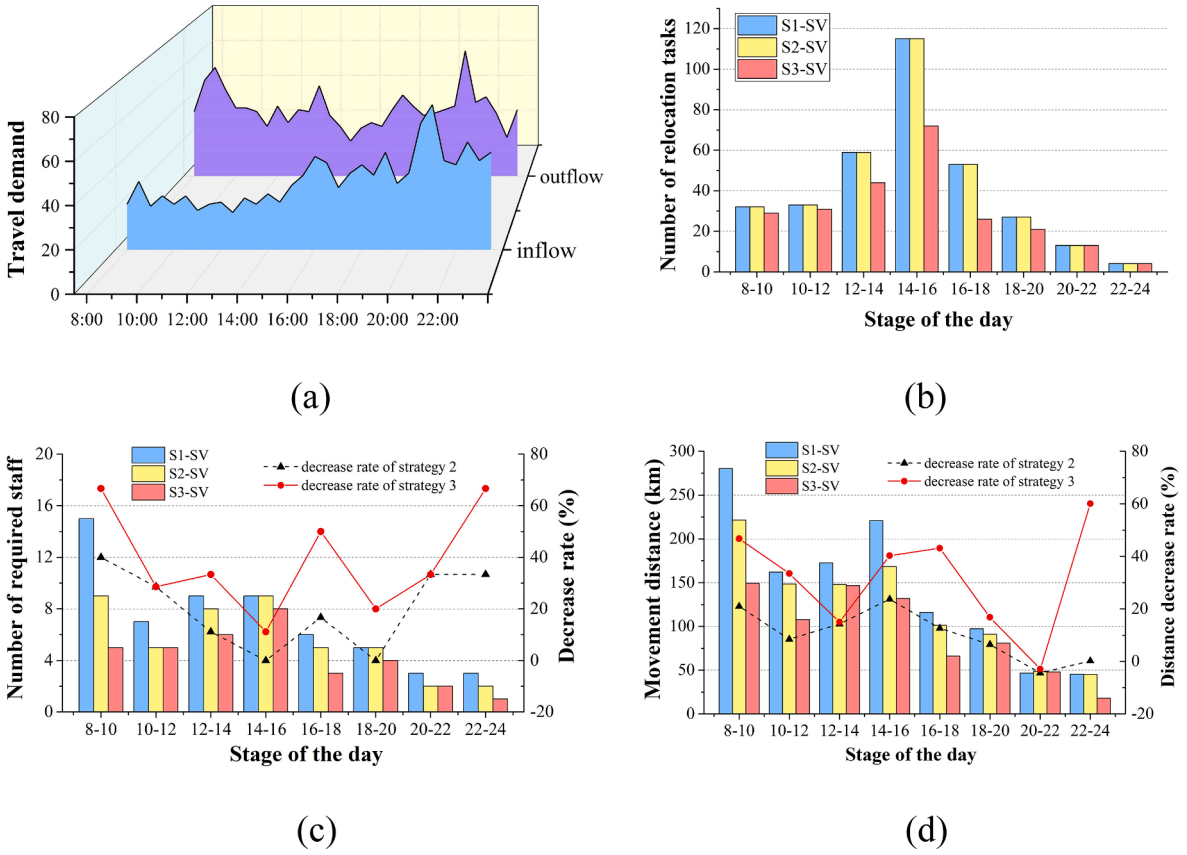

Fig. 13. Result comparison of three relocation strategies at different time periods: (a) Travel demand variation; (b) Number of relocation tasks; (c) Number of required staff; (d) Staff movement distance.

stations, although they may belong to different companies. The total relocation tasks are 240, and the vehicle relocation distance is greatly reduced to an average of 0.99 km per task. Therefore, the vehicle relocation costs in the Phase 1 model are $1,730.34, $1,730.34, and $715.26, respectively, for the three relocation strategies.

The relocation tasks obtained by solving the Phase 1 model serve as input to arrange the staff rebalancing routes in the Phase 2 model, which ensures that these relocation tasks can be performed. The relocation tasks in each company can only be performed by their own staff with S1-SV. However, the staff from different companies are considered to cooperate in relocation strategies S2-SV and S3-SV. Therefore, the staff are arranged to move to the nearby stations to perform relocation tasks although they may belong to different companies. On the one hand, the multi-company cooperative relocation reduces the number of staff. From the results of the

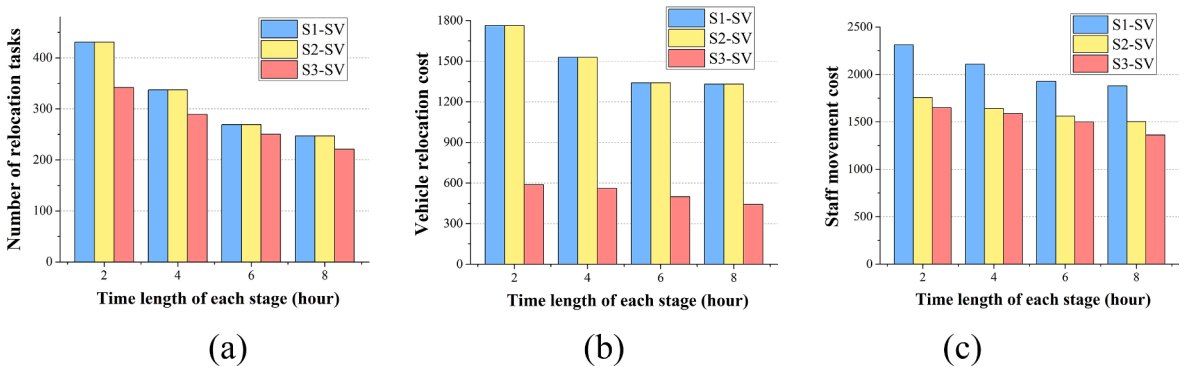

Fig. 14. Result comparison of three relocation strategies under different parameter settings on the rolling horizon method: (a) Number of relocation tasks; (b) Vehicle relocation cost; (c) Staff movement cost.

Phase 2 model in Table 5, we compare the number of required staff to perform the vehicle relocation tasks for each stage during the day. For the non-cooperative strategy S1-SV, the maximum number of required staff is 15, which means that at least 15 staff should be employed for the daily vehicle relocation. The cooperative strategy S2-SV requires nine staff, while the cooperative strategy S3-SV requires eight staff to accomplish the vehicle relocation tasks. On the other hand, the cooperative strategies decrease the staff movement distance. With the non-cooperative strategy S1-SV, the total daily staff movement distance is 1,141.25 km. However, this distance is reduced by 19.15% with the cooperative strategy S2-SV and 34.39% with the cooperative strategy S3-SV. In our model, if the relocation staff arrives at the target station and he/she has not yet reached the start of service time, waiting is required. We compare the staff's total waiting time with the three relocation strategies. The total waiting time during the day for non-cooperative strategy S1-SV is 1,802.43 min, while the total waiting time for cooperative strategy S2-SV and cooperative strategy S3-SV is 1,036.39 min and 763.66 min, respectively. Therefore, the cooperative relocation strategies can effectively reduce the number of staff, decrease the staff movement distance between stations, and improve the work efficiency of staff, avoiding them idling at the stations with no tasks to perform.

In Table 6, we analyze relocation results with three relocation strategies during the holiday (May 1st, 2018, Labor Day), where the pick-up demand and return demand in the carsharing system have significantly increased. In the results of the Phase 1 model, the vehicle relocation tasks are 431 with relocation strategies S1-SV and S2-SV. The corresponding average vehicle relocation distance is 1.34 km. With the relocation strategy with shared staff and vehicles S3-SV, 342 vehicle relocation tasks need to be performed, and the average vehicle relocation distance is 0.57 km. In the results of the Phase 2 model, in order to complete the relocation tasks, the maximum number of required staff by the three relocation strategies are 18, 13, and 10 respectively. With the cooperative relocation strategies, S2-SV and S3-SV, the staff have more degrees of freedom to perform the relocation tasks temporally and spatially. For example, the staff are arranged to perform the nearby and suitable relocation tasks, which avoids the staff idling time in stations and decreases the waste of distance in the vehicle relocation process and staff movement process. The total revenue has increased because of the larger travel demand for carsharing trips on holidays. Compared with the non-cooperative strategy S1-SV, the profit is increased by 6.08% with cooperative strategy S2-SV and is increased by 19.79% with cooperative strategy S3-SV.

At different time periods of the day, the users' pick-up demand and return demand in the carsharing system are imbalanced. At different stations, the inflow and outflow demands are quite diverse throughout the day. Fig. 13 shows the vehicle relocation and staff rebalance results with the three strategies at different time periods of the working day. In real-world stations, the total outflow demand is greater in the morning, whereas the total inflow demand in the afternoon is larger, as shown in Fig. 13(a), which is related to the land-use characteristics around these stations. Fig. 13(b) shows the relocation tasks required by solving the Phase1 model with three relocation strategies. More relocation tasks appear in the fourth period (14:00–16:00), which is caused by the gap accumulation of inflow and outflow demand. Fig. 13(c) shows the number of staff required to complete the relocation tasks. The improvement in the cooperation relocation is different during the day. For example, in the first period (8:00–10:00), adopting the cooperation relocation strategy S2-SV requires only nine staff. However, a total of 15 staff should be employed with the relocation strategy S1-SV. In the sixth period (18:00–20:00), the relocation strategy S2-SV requires five staff to complete the relocation tasks, which is the same as the relocation strategy S1-SV. The staff movement distance using the three relocation strategies is compared in Fig. 13(d). With the cooperation strategy, the staff will be arranged at the nearby stations to complete the vehicle relocation tasks. If the time window constraints are met, a small number of staff members will be used, and thus the total cost, including the vehicle relocation and staff movement can be effectively reduced.

We perform the sensitivity experiments with different parameter settings on the rolling horizon method to assess the effect on the number of relocation tasks, vehicle relocation cost, and staff movement cost. Fig. 14 shows the result comparison of the three relocation strategies with the holiday data. Both the vehicle relocation cost and the staff movement cost are reduced when the stage length is set longer. For example, when the stage length is set as 2 h, according to the results of the Phase 1 model, 431 relocation tasks should be completed and the total vehicle relocation cost during the day is $1,731.32 with relocation strategies S1-SV and S2-SV. When the stage length is set to 6 h, the number of relocation tasks is reduced to 269 and the vehicle relocation cost is $1,339.99. The rolling horizon approach can provide a better solution for vehicle relocation and staff rebalancing when more accurate travel demand

Table 7
The cooperative relocation strategies with the current SVs and future SAVs.

Relocation strategies	Description
S1-SV	the SV relocation without cooperation
S2-SV	the SV relocation with only shared staff
S3-SV	the SV relocation with shared staff and vehicles
S1-SAV	the SAV relocation without cooperation
S2-SAV	the SAV relocation with shared vehicles

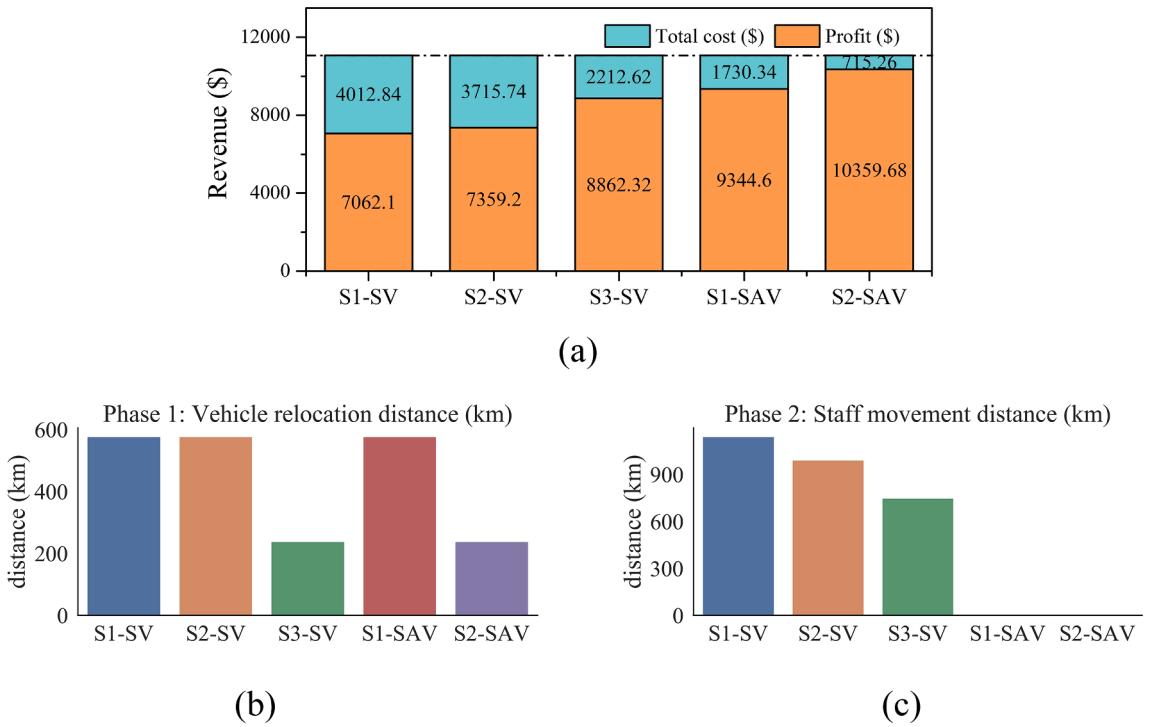

Fig. 15. Result comparison of different relocation strategies with SVs and SAVs: (a) Total cost and profit; (b) Vehicle relocation distance and (c) Staff movement distance.

predictions for the next time steps are available. The results of the rolling horizon method are suboptimal compared to considering the travel demand of the entire day, but calculating the optimal solution for an entire day is not a realistic objective because it is very difficult to accurately predict the travel demand for multiple time steps.

6.2.2. Future relocation with automated vehicles

In a scenario where shared automated vehicles (SAVs) are used, the cost of the entire system is only the vehicle relocation between stations. Using the model proposed in this study, we calculate the difference between the use of SAVs and current shared vehicles (SVs) in the carsharing system in terms of revenue and vehicle relocation cost on a working day. Table 7 shows the cooperative relocation strategies in the carsharing system, which includes the three aforementioned relocation strategies with current SVs and two relocation strategies with future SAVs. S1-SAV represents the relocation of SAVs without cooperative strategies, where vehicles from different companies can only be parked at the stations of specific companies. S2-SAV represents the cooperative relocation of multi-company SAVs, where the vehicles and parking stations of different companies are shared. As shown in Fig. 15 (a), under the same travel demand, the use of shared vehicles and shared staff can effectively increase the profit of the system, which focuses on reducing the vehicle relocation distance, the staff movement distance, and improving the work efficiency of staff. Compared with S1-SV, the profit increased by 6.19% and 25.49% with the cooperative relocation strategies S2-SV and S3-SV, respectively. In the SAV system, without the need for employing the relocation staff, the profits of S1-SAV and S2-SAV are $9,344.60 and $10,359.68, which is increased by 32.32% and 46.69% compared to the S1-SV in the current carsharing system. More detailed relocation results, such as vehicle relocation distance and staff movement distance for shared vehicles in the current SV system and the SAV system are shown in Fig. 15 (b) and (c).

Table A1
Results comparison of CPLEX and other heuristics.

Number of tasks	CPU/s	Instance	SA		TS		ACO		ALNS-ESA		CPLEX		ALNS-ESA vs SA	ALNS-ESA vs TS	ALNS-ESA vs ACO
			Best	Mean	Best	Mean	Best	Mean	Best	Mean	Best	CPU/s	Improvement	Improvement	Improvement
10	8	T10_1	55.29	55.36	55.29	57.50	55.29	55.94	55.29	55.29	55.29	0.48	0.13 %	4.00 %	1.18 %
		T10_2	101.76	102.01	101.76	101.76	101.76	104.22	101.76	101.76	101.76	0.52	0.25 %	0.00 %	2.42 %
20	20	T20_1	123.64	126.55	128.68	132.02	125.85	131.02	123.64	123.64	123.64	3.89	2.35 %	6.78 %	5.97 %
		T20_2	124.61	126.30	127.06	129.96	124.61	129.66	124.61	125.73	124.61	4.58	0.45 %	3.36 %	3.13 %
30	60	T30_1	164.68	171.37	175.36	175.36	170.18	176.25	147.67	149.46	146.48	17.54	14.66 %	17.33 %	17.92 %
		T30_2	210.29	214.79	215.45	218.01	235.51	240.47	205.99	208.73	205.99	16.36	2.90 %	4.45 %	15.21 %
40	100	T40_1	228.29	242.45	249.71	251.56	271.79	275.02	231.65	234.93	227.87	46.52	3.20 %	7.08 %	17.06 %
		T40_2	225.78	234.83	231.80	237.07	256.38	263.87	219.12	220.96	218.15	64.63	6.28 %	7.29 %	19.42 %
50	120	T50_1	263.91	283.09	290.46	292.30	286.33	294.06	258.81	259.65	258.22	75.90	9.03 %	12.57 %	13.25 %
		T50_2	314.13	320.03	352.91	354.39	342.67	354.26	302.45	306.95	301.43	102.85	4.26 %	15.46 %	15.41 %
60	180	T60_1	344.72	355.72	362.06	374.09	376.00	385.89	326.27	328.94	323.31	223.06	8.14 %	13.73 %	17.31 %
		T60_2	423.13	443.74	428.02	430.06	470.32	483.64	406.28	408.03	404.62	338.65	8.75 %	5.40 %	18.53 %
70	220	T70_1	464.24	496.63	468.27	471.19	496.98	516.58	429.55	431.88	426.50	2483.62	14.99 %	9.10 %	19.61 %
		T70_2	479.78	504.63	461.58	463.26	534.8	553.87	427.34	432.60	425.83	2631.35	16.65 %	7.09 %	28.03 %
80	250	T80_1	530.38	554.20	510.86	525.75	562.97	570.12	472.92	477.29	–	>3600	16.11 %	10.15 %	19.45 %
		T80_2	558.30	576.31	512.71	528.95	583.70	590.52	466.03	468.35	–	>3600	23.05 %	12.94 %	26.09 %
90	300	T90_1	632.31	660.92	539.46	575.11	628.11	642.40	497.86	504.81	–	>3600	30.92 %	13.93 %	27.26 %
		T90_2	654.37	705.74	598.03	623.17	675.93	691.43	532.40	538.93	–	>3600	30.95 %	15.63 %	28.30 %

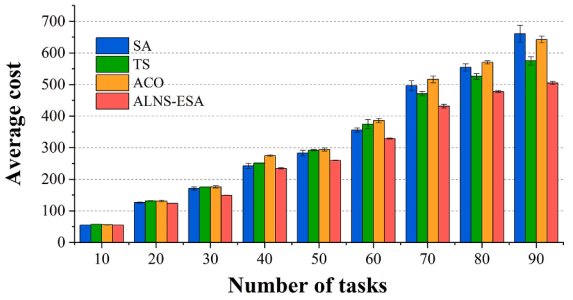

Fig. A1. Average cost comparison of different heuristics SA, TS, ACO, and ALNS-ESA.

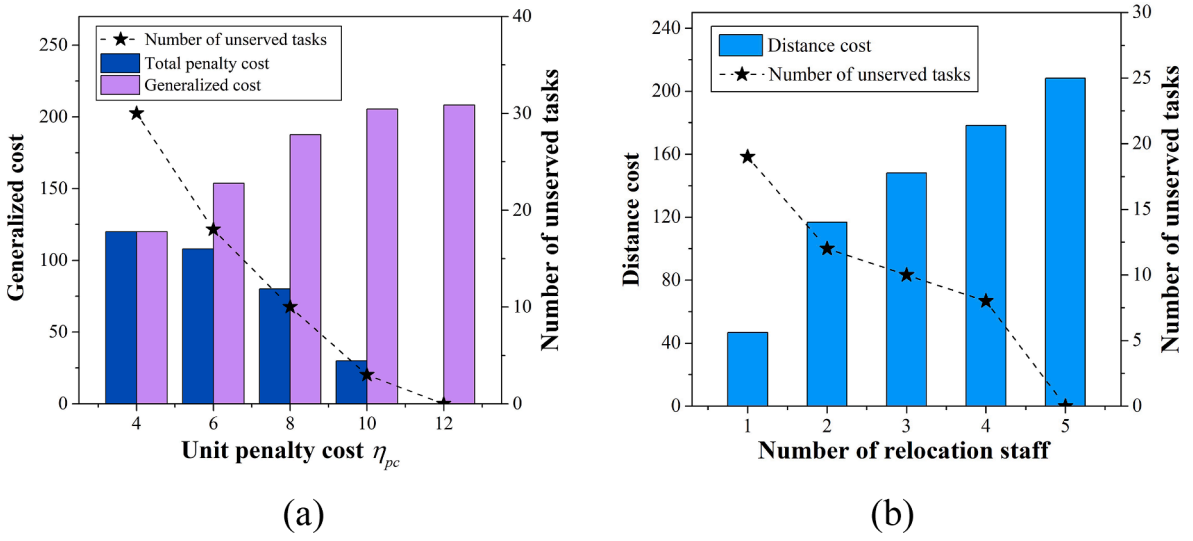

Fig. A2. The changes of generalized cost under different settings of parameters. (a) Unit penalty cost; (b) Number of relocation staff.

7. Conclusion and future studies

Carsharing is an emerging travel mode with potentially positive outcomes for mobility management in urban areas. Many carsharing companies have been established worldwide in the last decade. However, due to the large investment in buying vehicles and setting up stations, companies cannot be very large. The added management complexities in the carsharing business lead to customer loss and low vehicle utilization. Therefore, many carsharing companies are currently facing bankruptcy.

This study tackles the real-time vehicle relocation and staff rebalancing problem in the one-way carsharing systems with cooperative relocation strategies between different companies in a city. We propose a data-driven, dynamic, and cooperative method for vehicle relocation and staff rebalancing in one-way carsharing systems. The entire method starts from the multi-step travel demand prediction using deep learning algorithms, where the graph convolutional network (GCN) layer, gated recurrent unit (GRU) layer, and the attention mechanism are integrated to extract the features from temporal and spatial variables. With the predicted inflow and outflow demand, a two-phase integer programming model has been proposed to optimize the process of vehicle relocations and staff movements. Subsequently, multi-company cooperative relocation strategies are designed with the sharing of vehicles and staff to reduce the vehicle relocation distance, the staff rebalancing distance, and improve the work efficiency of staff. The Adaptive Large Neighborhood Search (ALNS) based heuristic embedded in the rolling horizon solution framework is used to solve the proposed model. Based on the 6-month carsharing travel records in Fuzhou, China, the results show that the cooperative relocation strategies can effectively increase the profit of the carsharing system by 25.49% and 19.79% on weekdays and holidays, respectively. We also look forward to the future relocation of automated vehicles. Without the participation of staff, the one-day profit is increased by 46.69% compared to the current situation in the carsharing system.

In this study, we assume that the companies are willing to participate in the cooperation, ignoring the reality of competitions and games among companies. For example, a larger carsharing company with more shared vehicles, stations, and staff may not be willing to cooperate with small companies. Companies on the verge of bankruptcy need to cooperate with large carsharing companies to increase the utilization of vehicles and stations. In addition, a fair revenue assignment mechanism is crucial for the cooperative relocation among different carsharing companies (Li et al., 2018). Further studies should consider the fairness of benefits allocation

from sharing resources so that it creates the right incentives for carsharing companies to collaborate.

CRediT authorship contribution statement

Ximing Chang: Methodology, Software, Formal analysis, Writing – original draft, Visualization, Writing – review & editing. **Jianjun Wu:** Conceptualization, Data curation, Methodology. **Gonçalo Homem de Almeida Correia:** Methodology, Writing – review & editing, Supervision. **Huijun Sun:** Writing – review & editing, Supervision. **Ziyan Feng:** Methodology, Writing – review & editing.

Declaration of Competing Interest

The authors declare that they have no known competing financial interests or personal relationships that could have appeared to influence the work reported in this paper.

Acknowledgments

This work was supported by the National Natural Science Foundation of China (Nos 91846202, 71890972/71890970), the Fundamental Research Funds for the Central Universities (No. 2021RC237) and the 111 Project (No. B20071).

Appendix A. Performance evaluation of the ALNS based heuristic

We design a set of illustrative numerical examples to evaluate the performance of the ALNS based heuristic (ALNS-ESA algorithm) in Table A1. The results are compared with the optimal result obtained using a high-performance commercial solver, i.e., CPLEX (12.10 Academic Version) and other heuristics, such as simulated annealing (SA), tabu search (TS), and ant colony optimization (ACO). The experiments have been conducted on a personal computer with Intel Core i7, 2.8 GHz CPU, and 8 GB of memory. The parameters of the CPLEX solver are set to the default value and the maximum time for solving the model is limited to 3600 s for all the examples. For the heuristics, each instance is run 10 times to calculate the average objective value and the best objective value within the same CPU time. We compared the improvement of the average objective value by the ALNS-ESA algorithm against the other three heuristic methods in percentage in Table A1. The parameters of the ALNS-ESA algorithm are set as follows: the reward parameters are $\varrho_1 = 100, \varrho_2 = 30,$ and $\varrho_3 = 10$ and the control parameter is $\rho = 0.6$. The algorithms use an initial temperature $T_{init} = 10^4$, and a cooling rate of $\tau = 0.998$.

In Table A1, the tested instances are grouped according to the number of tasks that varied from 10 to 90, and each group has two different instances. All four heuristics can obtain the best route with small-scale instances, such as T10_1, T10_2, T20_1, and T20_2. With the expansion of the instance scale, the CPLEX solver and the heuristics take a longer time to obtain the optimal solutions. For example, on the T50_1 dataset, the average objective value obtained by the ALNS-ESA algorithm is improved by 9.03%, 12.57 %, and 13.25 % compared with the SA, TS, and ACO algorithms, respectively, within the same computational time. For the large-scale instances, for example, T80_1, T80_2, T90_1, and T90_2, the CPLEX solver cannot obtain a feasible solution within the maximum computation time, whereas the ALNS-ESA algorithm can yield high-quality solutions, which perform better than the CPLEX and other heuristics. Fig. A1 shows that the average cost varies with the different number of tasks, where the error bars indicate the standard deviations of the objective values in the 10 running times. In small-scale instances, the heuristics can converge to the same optimal value. For large-scale instances, the fluctuations in multiple runs lead to larger standard deviations, while the proposed ALNS-ESA algorithm can still perform well.

In the Phase 2 model, the limited number of staff may lead to situations where some relocation tasks cannot be completed. Thus, the penalty cost for not performing one relocation task η_{pc} is thus introduced. The generalized cost of the Phase 2 model includes the rebalancing distance cost between tasks and penalty cost for not fulfilling relocation tasks. We compare the generalized cost under different settings of the unit penalty cost η_{pc} with the T30_2 dataset in Fig. A2 (a). The results demonstrate that more relocation tasks are performed with the setting of a larger unit penalty cost η_{pc}. For example, when the unit penalty cost is $\eta_{pc} = 12$, all relocation tasks are performed and the generalized cost only includes the distance cost. However, not all the relocation needs are met when the penalty cost η_{pc} is set to a small value. In these cases, the distance cost is much higher than the penalty cost, and thus the staff will not choose to serve those tasks with long relocation distances. Fig. A2 (b) shows the changes in distance cost with the different numbers of relocation staff using the T30_2 dataset. As the number of staff increases, more tasks are completed. When equipped with one staff member, 19 tasks cannot be completed, and penalty costs are incurred. When equipped with five staff members, all the 30 tasks can be performed.

References

Becker, H., Ciari, F., Axhausen, K.W., 2017. Modeling free-floating carsharing use in Switzerland: A spatial regression and conditional logit approach. Transp. Res. Part C: Emerg. Technol. 81, 286–299.

Boldrini, C., Bruno, R., Laarabi, M.H., 2019. Weak signals in the mobility landscape: car sharing in ten European cities. EPJ Data Sci. 8 (1), 7.

Boyacı, B., Zografos, K.G., Geroliminis, N., 2015. An optimization framework for the development of efficient one-way carsharing systems. Eur. J. Oper. Res. 240 (3), 718–733.

Boyacı, B., Zografos, K.G., Geroliminis, N., 2017. An integrated optimization-simulation framework for vehicle and personnel relocations of electric carsharing systems with reservations. Transp. Res. Part B: Methodol. 95, 214–237.
Bruglieri, M., Colorni, A., Luè, A., 2014. The relocation problem for the one-way electric vehicle sharing. Networks 64 (4), 292–305.
Bruglieri, M., Pezzella, F., Pisacane, O., 2017. Heuristic algorithms for the operator-based relocation problem in one-way electric carsharing systems. Discrete Optim. 23, 56–80.
Bruglieri, M., Pezzella, F., Pisacane, O., 2018. A two-phase optimization method for a multiobjective vehicle relocation problem in electric carsharing systems. J. Combin. Optim. 36 (1), 162–193.
Caballini, C., Sacone, S., Saeednia, M., 2016. Cooperation among truck carriers in seaport containerized transportation. Transp. Res. Part E: Logist. Transp. Rev. 93, 38–56.
Chang, X., Wu, J., Sun, H., et al., 2021. Relocating operational and damaged bikes in free-floating systems: A data-driven modeling framework for level of service enhancement. Transp. Res. Part A: Policy Pract. 153, 235–260.
Chen, T.D., Kockelman, K.M., 2016. Carsharings life-cycle impacts on energy use and greenhouse gas emissions. Transp. Res. Part D 47, 276–284.
Demir, E., Bektaş, T., Laporte, G., 2012. An adaptive large neighborhood search heuristic for the pollution-routing problem. Eur. J. Oper. Res. 223 (2), 346–359.
Duan, D., Wu, X., Si, S., 2021. Novel interpretable mechanism of neural networks based on network decoupling method. Front. Eng. 8 (4), 572–581.
Efthymiou, D., Antoniou, C., 2012, Waddell, P. Which factors affect the willingness to join vehicle sharing systems? Evidence from young Greek drivers. In: Transportation Research Board 91st Annual Meeting, Washington, DC, USA, 1–19.
Febbraro, A.D., Sacco, N., Saeednia, M., 2019. One-way carsharing profit maximization by means of user-based vehicle relocation. IEEE Trans. Intell. Transp. Syst. 20 (2), 628–641.
Folkestad, C.A., Hansen, N., Fagerholt, K., Andersson, H., Pantuso, G., 2020. Optimal charging and repositioning of electric vehicles in a free-floating carsharing system. Comput. Oper. Res. 113, 104771.
Gambella, C., Malaguti, E., Masini, F., Vigo, D., 2018. Optimizing relocation operations in electric carsharing. Omega. 81, 234–245.
Hao, S., Lee, D., Zhao, D., 2019. Sequence to sequence learning with attention mechanism for short-term passenger flow prediction in large-scale metro system. Transp. Res. Part C: Emerg. Technol. 107, 287–300.
Ho, S.C., Szeto, W.Y., 2014. Solving a static repositioning problem in bike-sharing systems using iterated tabu search. Transp. Res. Part E: Logist. Transp. Rev. 69, 180–198.
Hu, S., Chen, P., Xin, F., Xie, C., 2019. Exploring the effect of battery capacity on electric vehicle sharing programs using a simulation approach. Transp. Res. Part D: Transp. Environ. 77, 164–177.
Huang, K., An, K., Rich, J., Ma, W., 2020. Vehicle relocation in one-way station-based electric carsharing systems: A comparative study of operator-based and user-based methods. Transp. Res. Part E: Logist. Transp. Rev. 142, 102081.
Huang, K., An, K., Correia, G., Rich, J., Ma, W., 2021. An innovative approach to solve the carsharing demand-supply imbalance problem under demand uncertainty. Transp. Res. Part C: Emerg. Technol. 132, 103369.
Huo, X., Wu, X., Li, M., Zheng, N., Yu, G., 2020. The allocation problem of electric carsharing system: a data-driven approach. Transp. Res. Part D: Transp. Environ. 78, 102192.
Illgen, S., Hoeck, M., 2019. Literature review of the vehicle relocation problem in one-way car sharing networks. Transp. Res. Part B: Methodol. 120, 193–204.
Jian, S., Rashidi, T.H., Wijayaratna, K., Dixit, V., 2016a. A Spatial Hazard-Based analysis for modelling vehicle selection in station-based carsharing systems. Transp. Res. Part C: Emerg. Technol. 72, 130–142.
Jian, S., Rey, D., Dixit, V., 2016b. Dynamic optimal vehicle relocation in carshare systems. Transp. Res. Rec. 2567 (1), 1–9.
Jian, S., Rashidi, T.H., Dixit, V., 2017. An analysis of carsharing vehicle choice and utilization patterns using multiple discrete-continuous extreme value (MDCEV) models. Transp. Res. Part A: Policy Pract. 103, 362–376.
Jian, S., Rey, D., Dixit, V., 2019. An integrated supply-demand approach to solving optimal relocations in station-based carsharing systems. Netw. Spatial Econ. 19 (2), 611–632.
Jian, S., Liu, W., Wang, X., Yang, H., Waller, S.T., 2020. On integrating carsharing and parking sharing services. Transp. Res. Part B: Methodol. 142, 19–44.
Jorge, D., Correia, G., 2013. Carsharing systems demand estimation and defined operations: a literature review. Eur. J. Transp. Infrastruct. Res. 13 (3), 201–220.
Jorge, D., Correia, G., Barnhart, C., 2014. Comparing optimal relocation operations with simulated relocation policies in one-way carsharing systems. IEEE Trans. Intell. Transp. Syst. 15 (4), 1667–1675.
Ke, J., Feng, S., Zhu, Z., Yang, H., Ye, J., 2021. Joint predictions of multi-modal ride-hailing demands: a deep multi-task multi-graph learning-based approach. Transp. Res. Part C Emerg. Technol. 127 (3), 103063.
Kek, A., Cheu, R., Meng, Q., Fung, C., 2009. A decision support system for vehicle relocation operations in carsharing systems. Transp. Res. Part E: Logist. Transp. Rev. 45 (1), 149–158.
Klincevicius, M., Morency, C., Trépanier, M., 2014. Assessing impact of carsharing on household car ownership in Montreal, Quebec, Canada. Transp. Res. Rec. 2416, 48–55.
Li, X., Rey, D., Dixit, V.V., 2018. An axiomatic characterization of fairness in transport networks: Application to road pricing and spatial equity. Transp. Policy 68, 142–157.
Lin, L., He, Z., Peeta, S., 2018. Predicting station-level hourly demand in a large-scale bike-sharing network: A graph convolutional neural network approach. Transp. Res. Part C: Emerg. Technol. 97, 258–276.
Lu, Y., Wang, K., Yuan, B., 2021. The vehicle relocation problem with operation teams in one-way carsharing systems. Int. J. Prod. Res. 2021, 1–15.
Luo, Z., Qin, H., Zhang, D., Lim, A., 2016. Adaptive large neighborhood search heuristics for the vehicle routing problem with stochastic demands and weight-related cost. Transp. Res. Part E: Logist. Transp. Rev. 85, 69–89.
Nourinejad, M., Roorda, M.J., 2014. A dynamic carsharing decision support system. Transp. Res. Part E: Logist. Transp. Rev. 66, 36–50.
Nourinejad, M., Zhu, S., Bahrami, S., Roorda, M., 2015. Vehicle relocation and staff rebalancing in one-way carsharing systems. Transp. Res. Part E: Logist. Transp. Rev. 81, 98–113.
Oliveira, S., Bezerra, L., Stützle, T., Dorigo, M., Wanner, E., Souza, S., 2021. A computational study on ant colony optimization for the traveling salesman problem with dynamic demands. Comput. Oper. Res. 135, 105359.
Phan, M.H., Kim, K.H., 2016. Collaborative truck scheduling and appointments for trucking companies and container terminals. Transp. Res. Part B: Methodol. 86, 37–50.
Repoux, M., Kaspi, M., Boyac, B., Geroliminis, N., 2019. Dynamic prediction-based relocation policies in one-way station-based carsharing systems with complete journey reservations. Transp. Res. Part B: Methodol. 130, 82–104.
Santos, G., Correia, G., 2019. Finding the relevance of staff-based vehicle relocations in one-way carsharing systems through the use of a simulation-based optimization tool. J. Intell. Transp. Syst. 23, 583–604.
Schmöller, S., Weikl, S., Müller, J., Bogenberger, K., 2015. Empirical analysis of free-floating carsharing usage: The Munich and Berlin case. Transp. Res. Part C: Emerg. Technol. 56, 34–51.
Schiffer, M., Hiermann, G., Rüdel, F., Walther, G., 2021. A polynomial-time algorithm for user-based relocation in free-floating car sharing systems. Transp. Res. Part B: Methodol. 143, 65–85.
Shaheen, S.A., Cohen, A.P., 2013. Carsharing and personal vehicle services: worldwide market developments and emerging trends. Int. J. Sustainable Transp. 7 (1), 5–34.
Shaheen, S.A., Chan, N.D., Micheaux, H., 2015. One-way carsharing's evolution and operator perspectives from the Americas. Transportation 42, 519–536.
Shui, C.S., Szeto, W.Y., 2017. Dynamic green bike repositioning problem - a hybrid rolling horizon artificial bee colony algorithm approach. Transp. Res. Part D Transp. Environ. 60, 119–136.
Sohu News: Problems Faced by Carsharing, 2017. From https://www.sohu.com/a/165042056_99965252.

Sohu News: The development status of carsharing industry in China, 2018. From https://www.sohu.com/a/303018464_473133.
Sprei, F., Habibi, S., Englund, C., Pettersson, S., Voronov, A., Wedlin, J., 2019. Free-floating car-sharing electrification and mode displacement: travel time and usage patterns from 12 cities in europe and the united states. Transp. Res. Part D: Transp. Environ. 71, 127–140.
Sun, P., Veelenturf, L.P., Hewitt, M., Woensel, T.V., 2020. Adaptive large neighborhood search for the time-dependent profitable pickup and delivery problem with time windows. Transp. Res. Part E: Logist. Transp. Rev. 138, 101942.
Vateekul, P., Sri-iesaranusorn, P., Aiemvaravutigul, P., Chanakitkarnchok, A., Rojviboonchai, K., 2021. Recurrent neural-based vehicle demand forecasting and relocation optimization for carsharing system: a real use case in Thailand. J. Adv. Transp. 2021, 8885671.
Wan, L., Tang, J., Wang, L., Schooling, J., 2021. Understanding non-commuting travel demand of car commuters – insights from anpr trip chain data in cambridge. Transp. Policy 106, 76–87.
Wang, L., Zhong, H., Ma, W., Zhong, Y., Wang, L., 2020a. Multi-source data-driven prediction for the dynamic pickup demand of one-way carsharing systems. Transportmetrica B. 8 (1), 90–107.
Wang, T., Hu, S., Jiang, Y., 2020b. Predicting shared-car use and examining nonlinear effects using gradient boosting regression trees. Int. J. Sustainable Transp. 15 (12), 893–907.
Wang, N., Jia, S., Liu, Q., 2021. A user-based relocation model for one-way electric carsharing system based on micro demand prediction and multi-objective optimization. J. Cleaner Prod. 296, 126485.
Wei, L., Zhang, Z., Zhang, D., Leung, S., 2018. A simulated annealing algorithm for the capacitated vehicle routing problem with two-dimensional loading constraints. Eur. J. Oper. Res. 265 (3), 843–859.
Weikl, S., Bogenberger, K., 2013. Relocation strategies and algorithms for free-floating car sharing systems. IEEE Intell. Transp. Syst. Mag. 5 (4), 100–111.
Weikl, S., Bogenberger, K., 2015. A practice-ready relocation model for free-floating carsharing systems with electric vehicles – mesoscopic approach and field trial results. Transp. Res. Part C: Emerg. Technol. 57, 206–223.
Wu, J., Hu, L., Jiang, Y., 2021. Collaborative strategic and tactical planning for one-way station-based carsharing systems with trip selection and vehicle relocation. Transp. Lett. https://doi.org/10.1080/19427867.2021.2008176.
Xu, M., Meng, Q., 2019. Fleet sizing for one-way electric carsharing services considering dynamic vehicle relocation and nonlinear charging profile. Transp. Res. Part E: Logist. Transp. Rev. 128, 23–49.
Yang, S., Wu, J., Sun, H., Qu, Y., Li, T., 2021. Double-balanced relocation optimization of one-way carsharing system with real-time requests. Transp. Res. Part C: Emerg. Technol. 125, 103071.
Yu, D., Li, Z., Zhong, Q., Ai, Y., Chen, W., 2020. Demand management of station-based car sharing system based on deep learning forecasting. J. Adv. Transp. 2020, 8935857.
Zeng, G., Sun, Z., Liu, S., et al., 2021. Percolation-based health management of complex traffic systems. Front. Eng. 8 (4), 557–571.
Zhang, C., He, J., Liu, Z., Xing, L., Wang, Y., 2019. Travel demand and distance analysis for free-floating car sharing based on deep learning method. PLoS ONE 14 (10), e0223973.
Zhao, M., Li, X., Yin, J., Cui, J., Yang, L., An, S., 2018. An integrated framework for electric vehicle rebalancing and staff relocation in one-way carsharing systems: Model formulation and Lagrangian relaxation-based solution approach. Transp. Res. Part B: Methodol. 117, 542–572.
Zhao, L., Song, Y., Zhang, C., Liu, Y., Wang, P., Lin, T., Deng, M., Li, H., 2019. T-gcn: a temporal graph convolutional network for traffic prediction. IEEE Trans. Intell. Transp. Syst. 21 (9), 3848–3858.
Zhu, H., Luo, Y., Liu, Q., Fan, H., Song, T., Yu, W., Du, B., 2019. Multistep flow prediction on carsharing systems: a multi-graph convolutional neural network with attention mechanism. Int. J. Software Eng. Knowl. Eng. 29, 1727–1740.